LOCALIZING GROUND TRANSMITTERS USING AIRBORNE ANTENNA ARRAY

by

Mirghani Moutaman Daffalla

A Thesis presented to the Faculty of the
American University of Sharjah
College of Engineering
In Partial Fulfillment
of the Requirements
for the Degree of

Master of Science in
Mechatronics Engineering

Sharjah, United Arab Emirates

December 2020

Declaration of Authorship

I declare that this thesis is my own work and, to the best of my knowledge and belief, it does not contain material published or written by a third party, except where permission has been obtained and/or appropriately cited through full and accurate referencing.

Signed Mirghani Daffalla

Date 15/12/2020

Approval Signatures

We, the undersigned, approve the Master's Thesis of Mirghani Moutaman Daffalla

Thesis Title: Localizing-ground Transmitters Using Airborne Antenna Array

Date of Defense: 07/12/2020

Name, Title and Affiliation	**Signature**
Dr. Hasan Mir Professor, Department of Electrical Engineering Thesis Advisor	
Dr. Mamoun Abdel-Hafez Professor, Department Mechanical Engineering Thesis Co-Advisor	
Dr. Nasser Qaddoumi Professor, Department of Electrical Engineering Thesis Co-Advisor	
Dr. Lotfi Romdhane Professor, Department of Mechanical Engineering Thesis Committee Member	
Dr. Usman Tariq Assistant Professor, Department of Electrical Engineering Thesis Committee Member	
Dr. Mohammad Jaradat Program Coordinator, Mechatronics Engineering Graduate Program	
Dr. Lotfi Romdhane Associate Dean for Graduate Affairs and Research College of Engineering	
Dr. Sirin Tekinay Dean, College of Engineering	
Dr. Mohamed El-Tarhuni Vice Provost for Graduate Studies Office of Graduate Studies	

Acknowledgement

I would like to thank my advisors Dr. Hasan Mir, Dr. Mamoun Abdel-Hafez, and Dr. Nasser Qaddoumi, whose expertise was priceless, throughout my research stages. I would particularly like to acknowledge Dr. Mir for providing knowledge, guidance, as well as his continuous support and motivation. His insightful assessment and evaluation pushed me to do my best to refine and improve my work. I am deeply grateful for his great assistance, worthy discussion and suggestions.

I would like to thank all the professors and colleagues in the Mechatronics Engineering department. With their wonderful collaboration, my master courses were very insightful and I gained high values from their expertise and skills. Additionally, I sincerely would like to thank the American University of Sharjah for supporting me and sponsoring my M.Sc. studies, which had a huge positive impact in my career life.

I would also like to thank my friends Ahmed Osman, Omer Motasim, and Ahmed Tajelsir, for their wonderful support and encouragement through my research years. Their continuous support led me to complete this thesis successfully.

In addition, my biggest thanks to my family for all the support they have shown to me during all years of my study. They were always there for me. Special thanks to my mother who kept supporting and motivating me emotionally. Moreover, the biggest thanks to my father, without whom I would not have been able to complete this research. He guided me and assisted me with all stages of my research.

Dedication

To my family…

Abstract

A radio direction finder (RDF) estimates the direction of arrival (DOA) of a radio signal. It receives multiple copies of the signal by a multiple-element antenna array, making use of the characteristics of the received signals. Measurement of the DOA of the received signal is used to localize signals sources, such as radars, mobile phone devices, and RF beacons. This thesis aims to design and implement a direction finding (DF) system that can be integrated on a mobile aerial platform, such as an unmanned aerial vehicle (UAV), in order to localize ground transmitters. General background and concepts about DF systems, RF transmitters, DF applications, and localization have been illustrated and discussed within the thesis. Through the thesis, DF algorithms and techniques have been described and addressed. Comprehensive design approaches and requirements are also discussed in detail. Related hardware is discussed, presented, and simulated and their effects on the system integration is addressed. In order to complement the DF system on a UAV, navigation methods and geographical positioning of the UAV are presented in the thesis .

Keywords: ***Direction of Arrival, Direction Finding, MUSIC, Phased Array Antenna, UAV, Localization, Hardware Anomalies*****.**

Table of Contents

List of Figures

List of Tables

List of Abbreviations

ADC	Analog to Digital Converter
ADF	Automatic Direction Finder
AOA	Angle of Arrival
DF	Direction Finding/Finder
DFT	Discrete Fourier Transform
DOA	Direction of Arrival
DOD	Direction of Departure
FFT	Fast Fourier Transform
FPGA	Field Programmable Gate Array
GPS	Global Positioning System
IF	Intermediate Frequency
IMU	Inertial Measurement Unit
INS	Inertial Navigation System
KF	Kalman Filter
LO	Local Oscillator
MUSIC	Multiple Signal Classification
PA	Phased Array
RDF	Radio Direction Finding/Finder
RF	Radio Frequency
SNR	Signal to Noise Ratio
UAS	Unmanned Aerial System
UAV	Unmanned Aerial Vehicle

Chapter 1. Introduction

1.1. Overview

Radio Direction Finding is the procedure of determining the bearing of a transmitting Radio Frequency (RF) source [1]. Passive Direction Finding (DF) systems with non-rotating antennas generally have an array of spatially displaced antennas, which are known as a phased array antenna. A phased array can be electronically steered to vary the transmission or receiving directivity without the need for mechanical rotation. Typically, three or more antennas are required for unambiguous DOA estimation, and the accuracy of the estimation increases with the elements number [2].

Radio Detection And Ranging (Radar) is an active DF system that can determine range, direction, and velocity of the targets. Classic radar uses mechanical steering for tracking and localizing targets. The antenna in this case has a big reflector that is needed to be mechanically directed towards the target to be able to track it. On the other hand, modern tracking radars use electronic beam scanning to track targets. The reflector antenna in this case is replaced with an antenna array. However, the power consumption of such array is relatively high, and not convenient for airborne applications.

To solve these issues, research was conducted in passive radio direction finding systems. The direction of a transmitting source with respect to a platform, such as an aircraft, can be determined passively using the received signals' characteristics. For example, it can be done by comparing the time of arrival of two or more signals at two or more elements at certain distances from each other [3].

1.2. DF Applications

Direction of Arrival (DOA) has been an active research area because of its various public services as well as security and military applications [4]. Two of these applications are radio DF for navigation purposes and locating RF emitters. While radio direction finding for navigation purposes is losing its importance in the presence and spread of satellite navigation systems, the requirements to determine the location of RF emitters increases with the mobility of communication device [2].

Today, anyone might notice the spread of devices that use electromagnetic (EM) signals, particularly cell phones, which became a major medium of communication.

Research institutes and governmental entities have realized the capability of using EM signals for localizing the user/owner even if he is unconscious, such as in search and rescue tasks [5]. Accordingly, there are existing projects such as I-LOV [6] and WISECOM [7] for RF source localization in disaster zones for search and rescue missions.

Another application for DOA estimation is radio frequency monitoring (RFM), which uses the same technology as radio frequency identification (RFID). RFM has a huge research interest in spectrum management as it ensures an accurate and valid usage of the spectrum at both national and international levels. Furthermore, RFM provides protection of legal spectrum allocations against interference resulting from illegal use [8]. Illegal repeaters are installed by some of the end users without the consent of authorities. This is because repeaters are considered to be a cheap solution to low signal strength problems [8]. RFM has wide applications including localization of non-authorized transmitting sources, mitigation of jamming, spoofing detection, and searching for interference sources [2].

Automatic Direction Finding (ADF) is a terminology that is used to differentiate DF systems that require manual intervention to operate versus those that do not [2]. In the military area, ADF is usually installed on a mobile platform to determine its heading. An aircraft, ship, or tank can use similar technique to estimate the location of friendly or enemy transmitters. This may be used for tracking enemies or homing to the RF source [9]. Direction finding technology is used to locate enemy aircraft during flight, ground control stations, radars, and radio navigation aids. In airports, a Non-Directional Beacon (NDB) is used as navigation aid to aircraft more or less like a lighthouse beacon, while the onboard ADF instrument measures the direction of the NDB to adjust its heading.

1.3. Research Problem and Contribution

The importance of localizing ground transmitters is increasing in areas that lack the capability of satellite localization. Those areas can be forests (for search and rescue mission) or crowded cities (to find unauthorized transmitters) or hidden military bases. In localizing ground transmitters, the need to integrate a DF system in a mobile platform can be a key factor to locate moving/ hidden transmitters in areas that are not accessible

by typical aircraft and satellites. Specially in military, use of small UAVs equipped with DF systems would achieve the upper hand in intelligence warfare.

In this thesis, DF background, importance, and applications will be studied. Passive DF estimation concept will be discussed as well as some of the techniques that are used to measure phase difference between multiple copies of the same signal that are received by phased array elements to determine the DOA.

This research aims to set the guidelines to design and implement a passive DF system that can be integrated on a mobile airborne platform. In this thesis, a beam-forming and high-resolution Multiple signal classification (MUSIC) algorithm is used to estimate DOA in various conditions. Furthermore, the need to integrate DF systems with navigation systems will be discussed. In addition, the hardware design and implementation requirements will be addressed.

All scenarios will be simulated in MATLAB and Simulink with different test subjects including varying signal-to-noise ratio (SNR), hardware anomalies, RF anomalies, and other test criteria to investigate the performance of DF algorithm in airborne scenarios. Furthermore, the need to integrate DF systems with navigation systems will be discussed, and simulation tests will be done to measure the DF estimation performance in 3D space.

1.5. Thesis Organization

The rest of this document is arranged as follows: Chapter 2 reviews the background and literature related to antenna arrays, direction finding, navigation systems, and localization. Chapter 3 discusses the DF system model, passive DF concepts, the DOA estimation techniques, and geolocation approach. Chapter 4 shows the DF system hardware requirements, design guidelines, and proposes hardware solutions to implement the DF on an airborne platform. Chapter 5 introduces Simulink models and results for phase measurement algorithms, MUSIC estimation technique results, and introduces the hardware effects which was discussed in Chapter 4 and shows their simulation results. Chapter 6 concludes the entire research, and includes discussion and recommendations for potential future work.

Chapter 2. Background and Literature Review

2.1. Introduction

In this chapter, the fundamentals of direction-finding systems and phased Array systems will be discussed. In addition, different direction of arrival (DOA) estimation techniques will be presented, as well as the method to use the information they provide to geographically localize the transmitters using Unmanned Aerial Systems (UAS). Furthermore, Inertial Navigation System (INS) mechanism and how it can be used to localize moving platforms will be discussed.

2.2. Direction Finding Systems

DF systems are categorized on the basis of the methods used to evaluate the DOA of an emitter of interest such as: amplitude-based, phase-based, and time-based techniques. The two popular used methods in passive RDF transmitters localization are amplitude comparison and beam rotating [10]. The beam rotating techniques provide more accurate DOA estimation than amplitude comparison methods. However, it requires a larger number of antenna elements to achieve the automatic steering and obtain the maximum response of the acquired transmitter [10]. On the other hand, the amplitude comparison methods [11] [12] are cheaper and simpler. The DOA can be computed using only the amplitude of the received signals on two or more antenna elements. There is no steering process required for amplitude comparison methods. However, the accuracy of amplitude based systems is not as good as beam rotating methods due to the noise and distortion of antenna beam patterns, which leads to large deviation from the actual DOA [13].

Although the requirements might change between different DF systems, in general, a typical system basically consists of a DF antenna, DF receiver, DF bearing processor, and a DF bearing display. When a DF system is designed, each component is selected based on its specific purpose. However, each component should have a suitable interface for the integration. The most suitable pieces of equipment are selected by the manufacturer so as to meet the requirements. Selection depends on many factors, of which the first consideration is the cost of the components, then the size and weight of the hardware. The manufacturer may also consider the ease of use and the neatness of the system design [2].

2.3. Phased Antenna Array

2.3.1. Antennas. An antenna is a crucial device used by all the wireless communications, which rely on using antennas as transducers. Transducers convert electrical signals into electromagnetic waves, and vice versa. Functionally, an antenna is the device used to send information in the free space in the form of electromagnetic waves. Antennas are classified based on their application area, structure, frequency band of operation, directivity, and radiation pattern [14].

2.3.2. Antenna arrays. Antennas can be combined, and their received signals are processed together. The larger the number of antenna array elements, the more efficient and accurate results are obtained. Moreover, more directional or focused antenna can be designed using the array method. However, the complexity of the system increases, and the system load and the overall cost will increase accordingly.

Antenna arrays can be used to steer the transmitted energy in a specific direction by choosing the appropriate geometry and weights of its elements. Similarly, it can be used as a receiver to estimate the direction of the received signal. Figure 1.1 shows the receiver structure of *K* element antenna array.

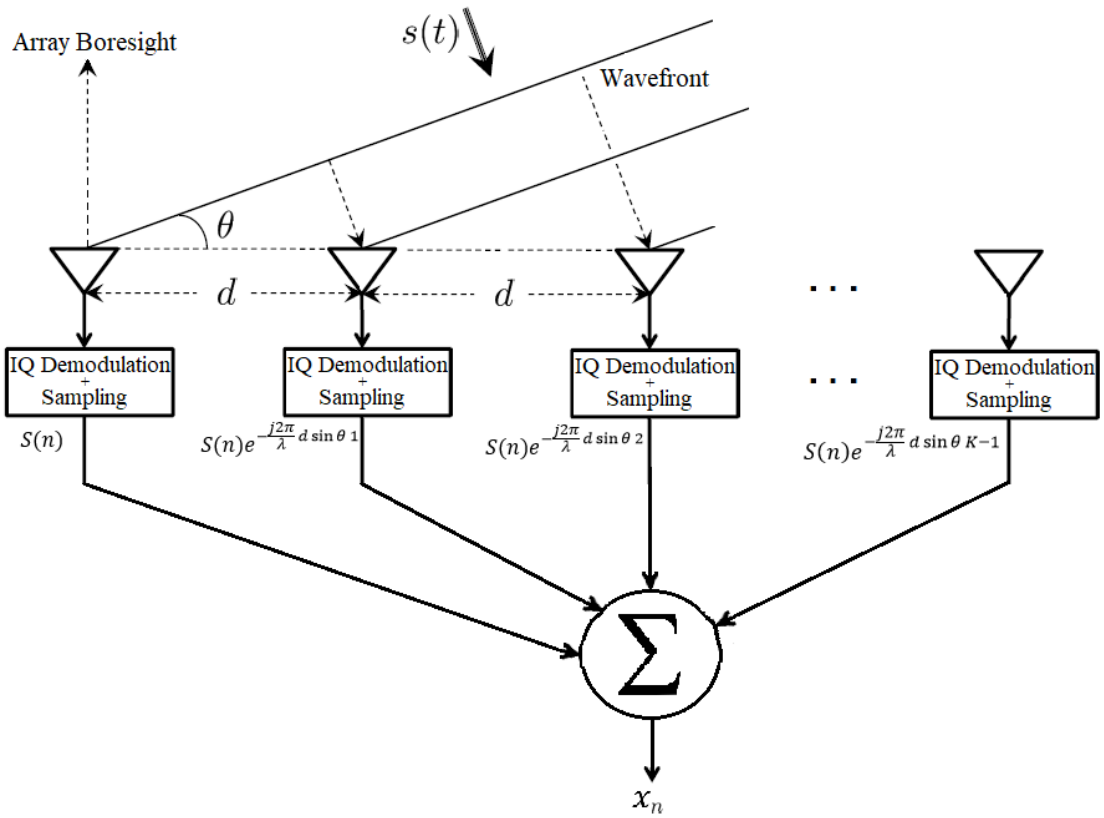

Figure 1.1: Antenna array receiver structure

2.3.3. Antenna array designs. Antenna arrays are classified based on the way the antenna elements are set. Some of the common geometry designs are uniform arrays such as uniform linear array (ULA), uniform circular array (UCA), and uniform rectangular array (URA).

The antenna array geometry decides the direction of transmission and reception of signals as well as the antenna beam pattern. One of the most used designs is the ULA, which consists of equally-spaced antenna elements arranged in a straight line [15].

2.3.4. Steering vector. By assuming the radiating RF source is in a far distance that is sufficient to make the wavefront approximately a plane wave, the received signals on the array elements can be described by a steering vector. For a radio plane wave received from a direction of arrival (θ), the steering vector $v_n(\theta)$ is a complex vector that describes the phase differences between the plane wave copies that are received on multiple elements of the antenna array. For a ULA with *K* elements, the steering vector is calculated as follows:

$$v_n(\theta) = \exp\left(-j\ 2\pi\ n \frac{d\ \sin(\theta)}{\lambda}\ \right), \quad n = 0, 1, 2, \dots, K \tag{2.1}$$

where d is the spacing between array elements and λ is the wavelength.

2.4. DOA Estimation Techniques

Generally, DOA estimation techniques are classified into conventional beamforming techniques, subspace-based methods, and maximum likelihood techniques [16]. In this section, some popular DOA estimation methods will be presented.

2.4.1. Power-based DOA estimation. Using an antenna array requires a complex receiver structure, since each array element (antenna), requires a separate receiver channel. Furthermore, the receiver channels are required to be coherent and the system should be well calibrated.

For low-cost applications, DOA estimation can be done using the knowledge of the signal power, which is known as the received signal strength indicator (RSSI). This requires prior knowledge of the antenna beam-pattern and the ability to estimate the unknown path loss as well as the transmit power of the signal [17].

Power-based DOA estimation can be done using several techniques. One way is to use directional antenna array elements pointing in different directions [18]. Another approach is by using a single antenna with an actuator to rotate the antenna and obtain measurements from different angles. However, actuators are mechanical parts that require maintenance. They also slow the update rate of information, and consume extra power to operate the system [19].

In power estimation techniques, the power of the received signal is measured while steering the antenna beam through steering vector calculations to find the maximum beam power.

Power-based DOA estimation methods suffer from poor resolution. If two radiating sources are near to each other (i.e., their respected DOAs are close to each other), then those techniques will not be able to distinguish between the two sources directions, and ambiguity in the beam pattern will occur. Figure 2.2 shows the resulting beam pattern for three DOAs (*30°,40°,70°*), as can be seen, the power-based estimation failed to distinguish between the first two DOAs.

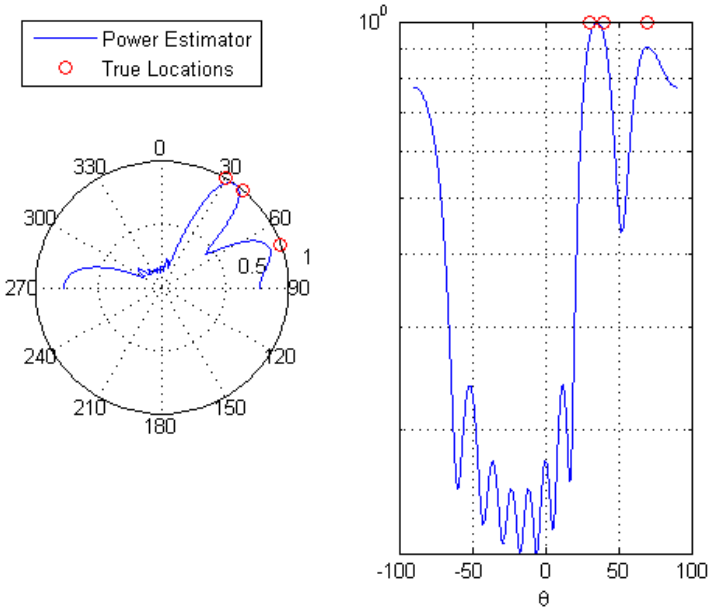

Figure 2.2: Power-based DOA estimation

2.4.2. Multiple signal classification (MUSIC). MUSIC algorithm was introduced by Schmidt as a high-resolution technique that can distinguish between closely spaced radiating sources. MUSIC estimates the number of incident waves with their DOA and provides a measurement of the signal strength as well [20].

MUSIC is based on exploiting the eigen-structure of the input covariance matrix. The algorithm decomposes the covariance matrix into eigen-vectors into the signal and noise subspaces. The direction of sources is calculated from steering vectors orthogonal to the noise subspace [20].

MUSIC promises to provide unbiased estimates of the number of signals, the angle of arrival, and the strength of the waveform. MUSIC makes the assumption that the noise in each channel is uncorrelated, making the noise correlation matrix diagonal. The incident signals may be correlated, creating a non-diagonal signal correlation matrix. However, under high signal correlation the traditional MUSIC algorithm breaks down and other methods must be implemented to avoid this weakness.

If the number of signals is *P*, the number of signals eigen-values and eigen-vectors is *D*, and the number of noises eigen-values and eigen-vectors is $M - P$ (where M is the number of antenna array elements). Because MUSIC exploits the noise eigen-vector subspace, it is sometimes referred to as a subspace method.

Assume multiple signals $\{s_{1,n}, \dots, s_{p,n}\}$, where *P* is number of the radiating sources, originated from directions $\{\theta_1, \dots, \theta_p\}$. The received signal model at instance *n* can be expressed as:

$$x_n = \sum_{p=1}^{P} s_{p,n} v(\theta_p) + u_n \tag{2.2}$$

where *v* is the steering vector obtained at angle θ_p, u_n is the additive noise received on each antenna element.

The first step in finding the DOA using MUSIC is to calculate the autocorrelation matrix, which is also known as the covariance matrix. By collecting *N* samples of the received signal x_n which was computed in Equation (2.2), the covariance matrix R_{xx} can be calculated using the formula

$$R_{xx} \approx \frac{1}{N} \sum_{n=0}^{N-1} x_n x_n^H \tag{2.3}$$

Next, the eigen-decomposition is computed for the matrix R_{xx} to find the eigenvectors and then the eigen-values. Thus,

$$R_{xx} = EAE^H \tag{2.4}$$

Then, by arranging the eigen-values, one can determine the number of the received signals and differ it from the interference subspace. Assuming P is the number of RF signals that were found, the interference subspace E_i can be written as follows

$$E_i = [E_{P+1}, E_{P+2}, \dots, E_M] \tag{2.5}$$

Finally, the DOAs can be estimated as the peaks of the spatial spectrum f. A steering vector v is used to scan the spectrum for $-90° \leq \theta \leq 90°$

$$f_{MUSIC}(\theta) = \frac{1}{\| v^H(\theta)\, E_i \|^2} \tag{2.6}$$

MUSIC algorithm is relatively complex due to the spectral search step, which has high computational complexity [21]. Hence, several modifications to the technique were developed to tackle the previously mentioned issues. However, classic MUSIC still widely used due to its good performance. Figure 2.3 shows the resulting beam pattern for three DOAs (*30°*,*40°*,*70°*), as can be seen, MUSIC was able to distinguish between the nearly spaced sources.

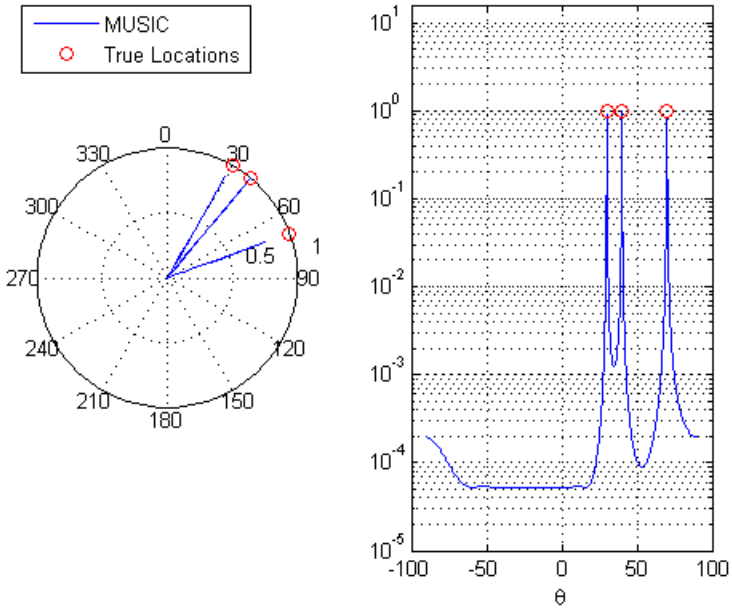

Figure 2.3: MUSIC DOA estimation

2.4.3. Root-MUSIC based DOA estimation. MUSIC algorithm is computationally complex and the cost of implementing it in the real world is extremely expensive [22]. To reduce this complexity, root-MUSIC algorithm was developed as

an efficient search-free adjustment to the original MUSIC algorithm [23]. Root-MUSIC finds the polynomial roots of the MUSIC instead of searching the full spectrum.

Root-Music approach reduces MUSIC computations, but it can only be applied to systems with uniform linear arrays (ULAs), whose sensors are distributed in a uniform grid. Several alternatives to the algorithm were proposed in [24] and [25].

Compared to MUSIC, root-MUSIC is considered more accurate and straightforward. For M-element ULA, the steering vector $v(\theta)$ is given as:

$$v(\theta) = p(z) = [1, z, \ldots, z^{M-1}]^T \tag{2.7}$$

where $z = e^{jw}$. After calculating the covariance matrix and finding the interference subspace, the polynomial of root-MUSIC can be written as:

$$f(z) = p^H(z) E_i E_i^H p(z) \tag{2.8}$$

This polynomial finds the *L* roots closest to the unit circle and estimates received signal DOAs as:

$$\theta_i = \arcsin\left(\frac{\lambda}{2\pi d} \arg\{z_i\}\right) \tag{2.9}$$

where z_i; $i = 1,2, \ldots, L$ are the closest roots to the unit circle.

2.4.4. ESPRIT algorithm. ESPRIT refers to Estimation of Signal Parameters via Rotational Invariance Technique. ESPRIT DF estimation approach is to exploit the rotational invariance in the received signal subspace, which is generated by two arrays with a translational invariance structure [26]. ESPRIT inherently assumes narrow-band signals so that one knows the translational phase relationships between the multiple arrays to be used. Similar to the MUSIC approach, ESPRIT assumes the RF signal sources are at a sufficient range from the receiving system so that the incident propagating field is nearly planar. Generally, the noise signal is assumed to be random with zero mean.

ESPRIT is computationally more efficient than MUSIC [27]. However, since it also uses the signal and noise subspace, it involves the estimation of the covariance matrix and its corresponding eigen-decomposition, which are computationally complex.

2.4.5. Test of orthogonality of projected subspaces (TOPS). Most of the classic DOA estimation techniques depend on maximum-likelihood. On the other hand, the subspace methods are applicable only to narrowband signals, in which energy is concentrated in a small frequency band as compared with the carrier frequency [28]. Subspace methods cannot be applied on wideband signals, since the phase difference between antennas does not depend only on the DOA; but also affected by the temporal frequency. Proposed solutions suggest that to decompose the wideband signal to narrowband signals using discrete Fourier transform (DFT). The DFT decomposition generates a collection of narrowband signals of different frequencies and the corresponding correlation matrices [29].

TOPS algorithm does not require the alignment between the signal and noise subspaces to create the covariance matrix. It determines if a DOA dependent transformation can achieve this alignment. TOPS do not cohere the signal and noise subspaces over frequency to achieve high processing gain. Applying multiple alignment tests over frequency leads to a more robust estimation at lower SNR compared to incoherent algorithms [28]. Not only TOPS is not affected by bias at high SNR, it also integrates frequency more efficiently at low SNR. Moreover, TOPS do not require beamforming matrix or focusing angles.

2.4.6. IQ demodulation technique. Quadrature modulation is a technique of combining two amplitude-modulated carrier signals in such a way that the original amplitude modulations are separable, by coherent demodulation, at the receiver.

A more sophisticated modulation technique that performs smoothly in digital processes is called IQ Modulation, where "I" stands for "in-phase" component of the signal, and "Q" stands for the "quadrature" component. In its different implementations, IQ modulation is an efficient way to exchange data, and it also operates well with digital formats. IQ modulation also eliminates phase measurement ambiguity [30].

IQ demodulation can be used to easily find the phase difference between sinusoidal signals. By applying it to the received signal at channel A and the delayed copy of the signal which is received at channel B, the phase difference can be found and hence the DOA can be estimated using the wave length and distance between the antennas.

Assume two received signals $s_1(t)$ and $s_2(t)$ at channel 1 and channel 2, where $s_2(t)$ is a delayed version of $s_1(t)$, such that

$$s_1(t) = A\cos\left(\omega_0\left(t - T_p\right) + \phi_{T_x}\right) \tag{2.10}$$

$$s_2(t) = A\cos\left(\omega_0\left(t - T_p - \tau\right) + \phi_{T_x}\right) = A\cos\left(\omega_0\left(t - T_p\right) + \phi_{T_x} - \omega_0\tau\right) \tag{2.11}$$

$$\phi = \omega_0\tau \tag{2.12}$$

where T_p represents the propagation time delay from the source to CH1, τ represents the time delay of the signal to propagate to channel 2, ϕ represents the phase difference between the two signals in radians.

IQ demodulation is applied to each received channel using the same oscillator (or coherent oscillators with the same frequency and phase, i.e. synchronized), which have the same frequency as the transmitted signal. Assume the oscillator signal $L(t)$ is:

$$L(t) = \cos(\omega_0 t + \phi_{Lo}) \tag{2.13}$$

where ϕ_{Lo} represents the oscillators phase shift.

Forming the IQ Signals: CH1 received signal is mixed with the oscillators signal to produce the mixer signal $M(t)$:

$$M(t) = s_1(t) * L(t) = A\cos\left(\omega_0\left(t - T_p\right) + \phi_{T_x}\right) * \cos(\omega_0 t + \phi_{Lo}) \tag{2.14}$$

$$M(t) = \frac{1}{2}A\cos\left(\omega_0 T_p - \phi_{T_x} + \phi_{Lo}\right) + \frac{1}{2}A\cos(2\omega_0 t - \omega_0 T_p + \phi_{T_x} + \phi_{Lo}) \tag{2.15}$$

The mixers output is filtered using a low pass filter. Hence, only the low frequency component will be obtained:

$$I = \frac{1}{2}A\cos\left(\omega_0 T_p - \phi_{T_x} + \phi_{Lo}\right) \tag{2.16}$$

CH1 received signal is also mixed with the oscillators shifted signal (π/2 shift), i.e. the Q signal, and then filtered to obtain the low frequency component. The Q signal will be found as:

$$Q = \frac{1}{2}A\sin\left(\omega_0 T_p - \phi_{T_x} + \phi_{Lo}\right) \tag{2.17}$$

The final step is combining the I and Q signals to obtain the channel output:

$$IQ_1 = I + jQ = \frac{1}{2}A\cos\left(\omega_0 T_p - \phi_{T_x} + \phi_{Lo}\right) + j\frac{1}{2}A\sin(\omega_0 T_p - \phi_{T_x} + \phi_{Lo}) \quad (2.18)$$

$$IQ_1 = \frac{1}{2}A\exp\ (j(\omega_0 T_p - \phi_{T_x} + \phi_{Lo})) \quad (2.19)$$

By following the same steps for CH2 demodulation, we can obtain the demodulated signal IQ_2 as:

$$IQ_2 = \frac{1}{2}A\exp\ (j(\omega_0 T_p + \omega_0\tau - \phi_{T_x} + \phi_{Lo})) \quad (2.20)$$

Phase Difference Measurement: Next, the IQ signals are multiplied, and the resulting complex value of this combination is as follows:

$$IQ = \overline{IQ_1} * IQ_2 \quad (2.21)$$

$$IQ = \frac{1}{2}A\exp(-j(\omega_0 T_p - \phi_{T_x} + \phi_{Lo}) * \frac{1}{2}A\exp(j\left(\omega_0 T_p + \omega_0\tau - \phi_{T_x} + \phi_{Lo}\right) \quad (2.22)$$

$$IQ = \frac{1}{4}A^2\exp(j\omega_0\tau) \quad (2.23)$$

It can be noticed that the phase of the complex IQ signal is the phase difference between the two signals, and since the signals frequency is known, then the time delay can be found and hence the DOA can be estimated.

$$\phi = \omega_0\tau = \measuredangle(IQ) \quad (2.24)$$

2.4.7. DFT method. Measuring the phase difference of two signals can be carried out using frequency characteristics. The classical method relies on zero-crossing detection [31][32], virtual vector voltmeter, on DFT [33] and on sine-wave fit methods [34]. These methods differ in their sensitivity towards non-coherent sampling.

Discrete Fourier Transform (DFT) is computed for *N* signal samples, and its spectrum is discrete in frequency and periodic with period *N*. The DFT can be found by sampling the Discrete-Time Fourier Transform (DTFT) spectrum, which is continuous and function of angular frequency ω.

The phase difference between the two measured signals can be found as the difference between the fundamental harmonics DFT phase spectra of those signals [33]. The DTFT spectrum of discrete time signals of length *NT* is

$$V_i\left(e^{j\omega T}\right) = \sum_{n=0}^{N-1} v_i(nT)(\cos(\omega nT) - j\sin(\omega nT)) \quad (2.25)$$

The DFT spectrum can be formed by sampling the DTFT at angular frequency $\omega_k=k\times(\omega_s N)$, hence

$$V_i(k) = \sum_{n=0}^{N-1} v_i(nT)(\cos\left(\frac{k\omega_s}{N}nT\right) - j\sin\left(\frac{k\omega_s}{N}nT\right)) \qquad (2.26)$$

Then, the phase difference of two sinusoidal signals v_1 and v_2 can be found as:

$$\phi_i = \arctan\frac{\mathrm{Im}(V_i(e^{-j\omega_k T}))}{\mathrm{Re}(V_i(e^{-j\omega_k T}))} = \frac{\sum_{n=0}^{N-1} v_1(nT)\sin(\frac{2\pi}{N}nk)}{\sum_{n=0}^{N-1} v_2(nT)\cos(\frac{2\pi}{N}nk)} \qquad i = 1,2 \qquad (2.27)$$

2.5. Navigation System

Since the objective of this study is to install a DF system on a mobile platform (like UAV), the information about direction of arrival is not enough. This can be attributed to the fact that the platform is not fixed in a specific geographical location, and extra information about the platform coordinates is required. Navigation systems are used to determine the position of a platform with respect to a known reference [35]. They often use gyroscopes, accelerometers, and radio receivers.

Navigation systems can be autonomous, such as Inertial Navigation System (INS) or dependent on external sources such as Global Navigation Satellite System (GNSS) like Global Positioning System (GPS). These two systems can be combined using the technique of Kalman filtering, which was principally developed for space navigation [36].

Autonomous systems (also known as dead-reckoning systems) depend on the knowledge and measurements of the starting location, velocity, and heading information. Position fixing systems relies on external sources with previously known location such as GPS and active beacons.

Dead-reckoning systems solution is based on previous measurements; thus, it is always available. However, errors can accumulate because the system is based on integration.

On the other hand, position fixing systems solution does not rely on previous positions since the information is obtained from external source. However, the solution is not always available since the external signal can be interfered or lost.

2.5.1. Global positioning system (GPS). GPS is a navigation system based on multiple satellites to provide accurate geographical location for civil and military uses [35]. GPS is independent of previous positions estimation since its signal is an externally updated signal.

However, it is not always convenient for applications that requires guaranteed solution due to its low update rate, and its signal can be lost because of the clouds, interference, jamming, or even spoofing.

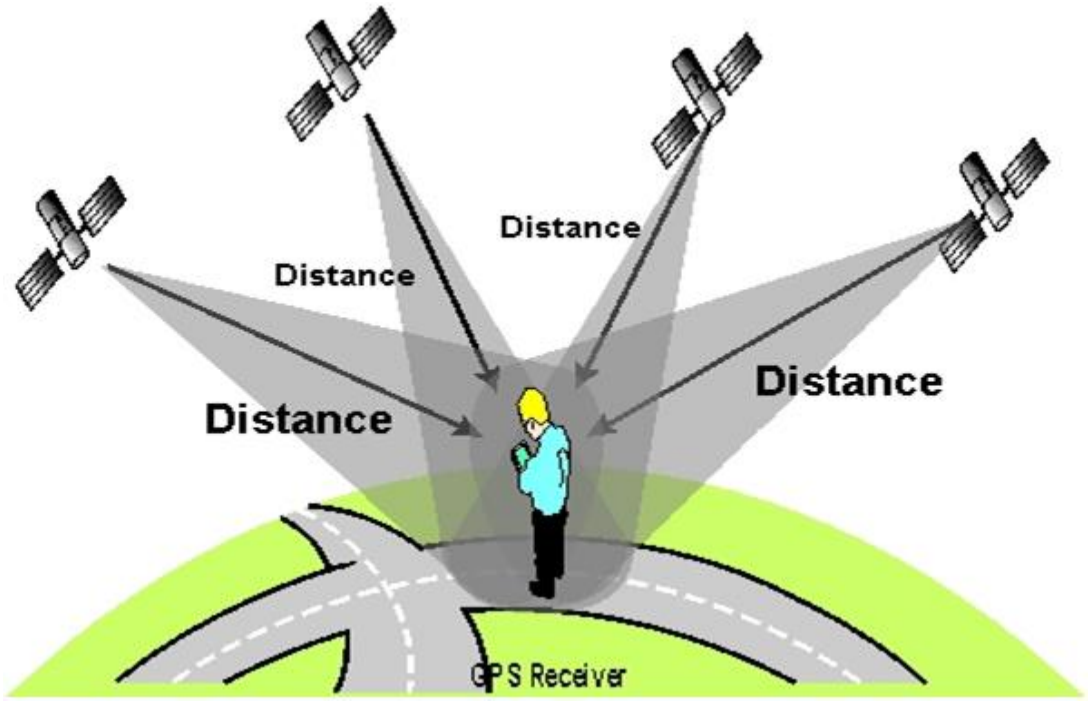

Figure 2.4: GPS localization [37]

2.5.2. Inertial navigation system (INS). INS use inertial measurement unit (IMU) which consists of gyroscopes and accelerometers with the related electronics [38]. Accelerometers measure acceleration and the INS algorithm integrates it to find velocity and position. Gyroscopes measure angular rates to estimate attitude information in the three dimensions. Using initial values of position, angular pose, velocity and attitude. Alongside the gravity model, the IMU processor keeps updating the current position, velocity and attitude of the platform. Linear motion in the three orthogonal directions is measured using accelerometers, while the angular motion is measured using gyroscopes. Figure 2.5 shows the basic components of the INS.

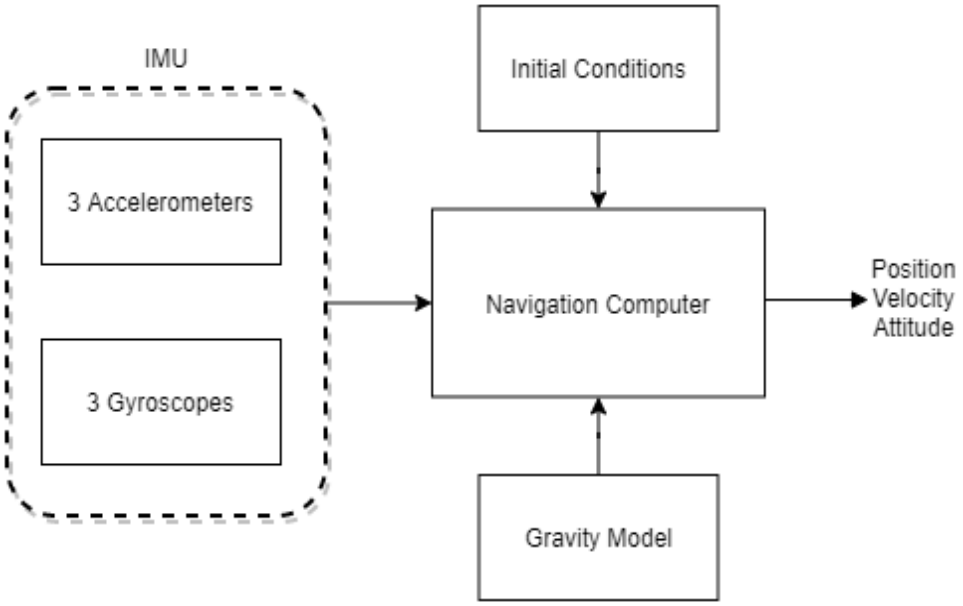

Figure 2.5: Inertial navigation system (INS) block diagram

Mechanization of INS is the process of converting the output of an IMU into position, velocity and attitude information. The outputs include rotation rates about three body axes measured by the gyroscopes triad. Additionally, the outputs include three specific forces along the body axes measured by the accelerometer triad all of which are with respect to the computational frame. Mechanization of INS is a recursive process that starts with a specified set of initial values and iterates on the output [39]. A general diagram of INS mechanization is shown in Figure 2.6.

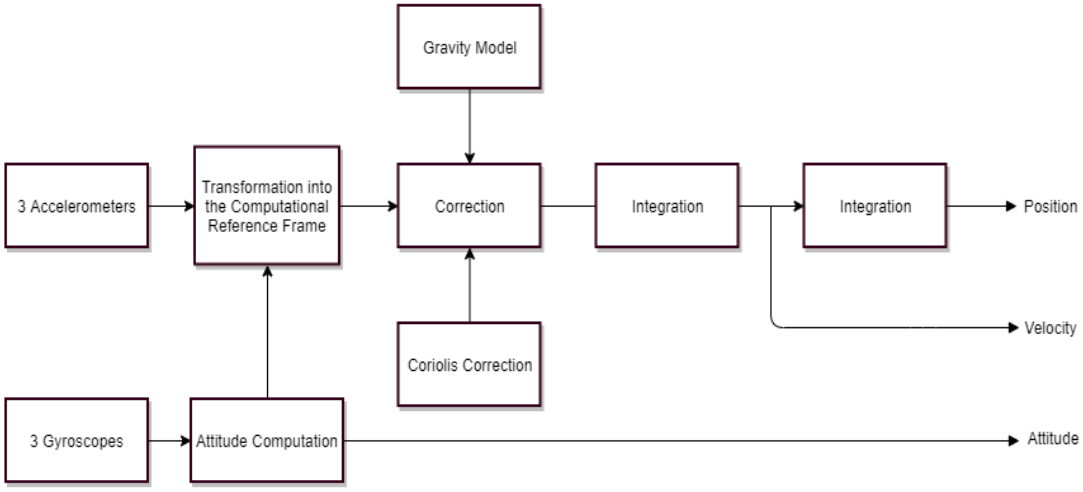

Figure 2.6: INS mechanization block diagram

2.5.3. Kalman filter. Kalman filter (KF) is one of the most effective data fusion algorithms. It is used in global positioning system receivers, phased-locked loops in radio equipment, smoothing noisy data and estimating parameters from multiple sensors' readings [40].

Due to the integration involved in the INS algorithm, the solution tends to drift with time, which leads to accumulation of error. Therefore, INS is often fused with other aided systems such as Camera, GPS, and SONAR. These aiding systems limit the error and predict the system behavior.

Kalman filter algorithm is used to fuse these systems by taking all the measurements from INS and the aided systems to produce more accurate estimation of the position. Figure 2.7 shows the simplified version of the Extended Kalman Filter which was proposed in [36]. The closed-loop configuration limits the error and supports the linearity for the KF technique.

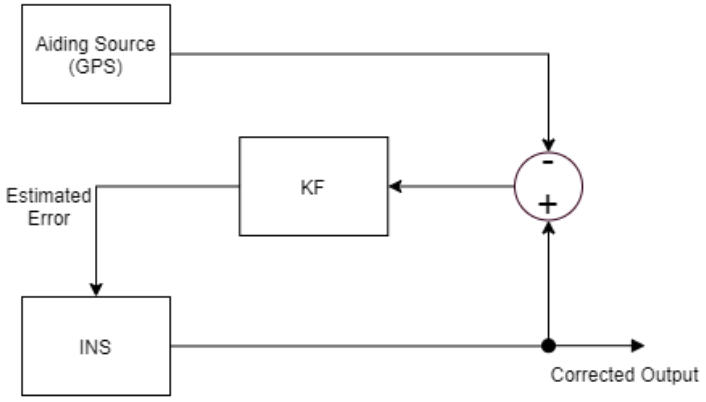

Figure 2.7: Extended Kalman filter block diagram

2.6. Coordinate Frames

A coordinate frame, in geometry, is an axes system that is used to uniquely describe the position of points or objects in an environment. In many applications, there are usually multiple coordinate frames that are used to correctly determine the position. Navigation algorithms require the knowledge of coordinate frames and how to transform between them.

To have a better understanding, we can consider this example. INS measures position and attitude based on its inertial frame which is fixed to the body of the vehicle that carries the inertial system. However, for most application, the information is

needed with respect to the Earth frame, and hence, it must be properly converted to a known Earth-fixed frame [39]. Figure 2.8 shows the main coordinate frames that are used in navigation systems.

2.6.1. Earth-centered inertial (ECI) (i-frame). The ECI coordinate frame origin is fixed at the center of mass of the Earth and its axes do not rotate with the Earth. ECI frames are named inertial and it is limited by gravitational field.

2.6.2. Earth-centered earth-fixed (ECEF) (e-frame). Also called ECR frame (earth-centered rotational frame), with its origin fixed to the Earth center. It is a Cartesian coordinate system which represents X, Y, and Z coordinates. The Z-axis is pointing to the North Pole, and the X-axis intersects between the equator and the Greenwich meridian planes. The Y-axis is orthogonal to both X and Z axes, and it can be found by the right-hand rule. The earth center of mass is considered as point (*0, 0, 0*) [41].

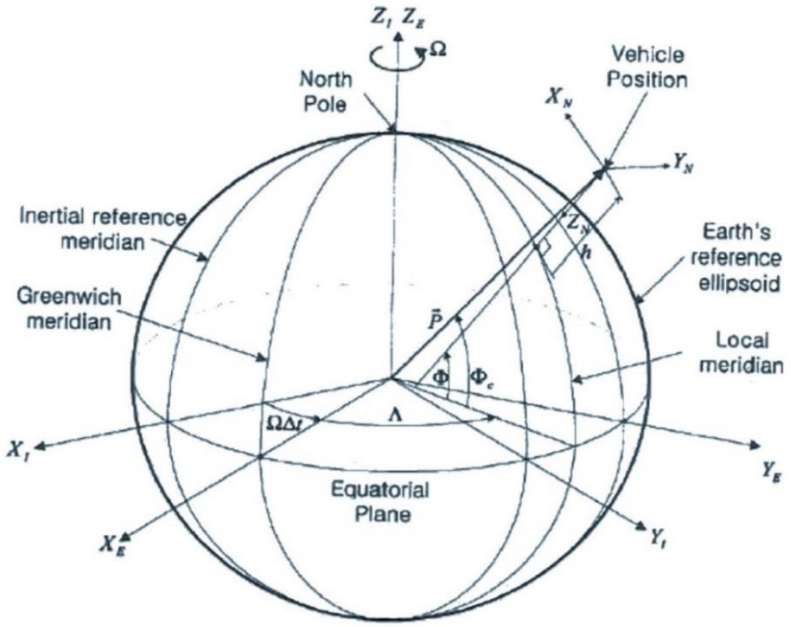

Figure 2.8: Axes systems [39]

2.6.3. Navigation frame (n-frame). This is the coordinate frame related to the inertial navigation system. Its origin is the location of the INS on the vehicle. It is also known as NED frame, meaning North-East-Down frame. The X-axis is pointing to the North Pole, Y-axis pointing to the east, and Z-axis is orthogonal to both axes and pointing down.

2.6.4. Body frame (b-frame). This frame is fixed to the vehicle, and its origin is the center of mass of its body. The X-axis points to the front of the vehicle. The Y-axis is orthogonal onto the X-axis and pointing to the right of the vehicle. Lastly, the Z-axis is perpendicular to both axes pointing upwards of the vehicle.

This frame is also described by the Euler angles. Elevation angle is around the Y-axis; which is nose down or up. Azimuth angle is around the Z-axis; which is nose right or left. Roll angle describes the rotation around the X-axis [42]. Figure 2.9 shows the body frame rotations expressed using Euler angles.

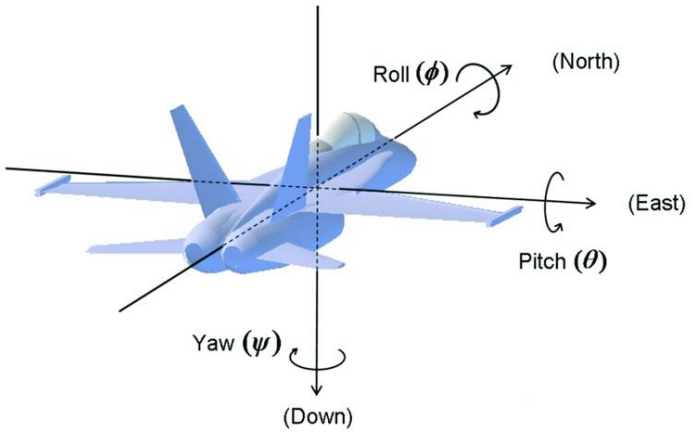

Figure 2.9: Pitch, roll, and yaw frames in an aircraft [43]

2.7. Unmanned Aerial Systems

Unmanned Aerial System (UAS) refers to the system that include the aircraft, communication units, and ground control. Unmanned Aerial Vehicle (UAV) can be defined as a "device used or intended to be used for flight in the air that has no-onboard pilot" [44]. UAVs provide aerial surveillance and close-up imagery in friendly as well as enemy areas since they are hard to detect with radars [45].

Currently, their applications include pipeline inspection, power lines inspection, traffic monitoring, emergency responses, search and rescue mission, environmental monitoring, aerial photography, imaging and mapping, chemical spraying, crop dusting and surveillance [46].

System load, hardware specifications as well as mission type must be considered when choosing a UAV platform. This is due to the fact that they have light weight and cannot carry heavy loads or fly for long time missions. These criteria will be considered in the design of the DF system with antenna array.

Chapter 3. System Modeling and Problem Formulation

This chapter discusses the passive DF system model and the received signal model, together with its phase relation to the DF. The MUSIC DOA estimation will be analysed and the guidelines for its implementation will be addressed. In addition, the need to integrate DF systems with navigation systems will be discussed.

3.1. DF System Model

Based on the research objective stated in Chapter 1, the DF system will be mounted on a UAV platform in order to localize ground transmitters. The DF system should be installed on the bottom of the drone to avoid interference that can be caused by the propellers. Figure 3.1 shows the conceptual structure of the integrated system.

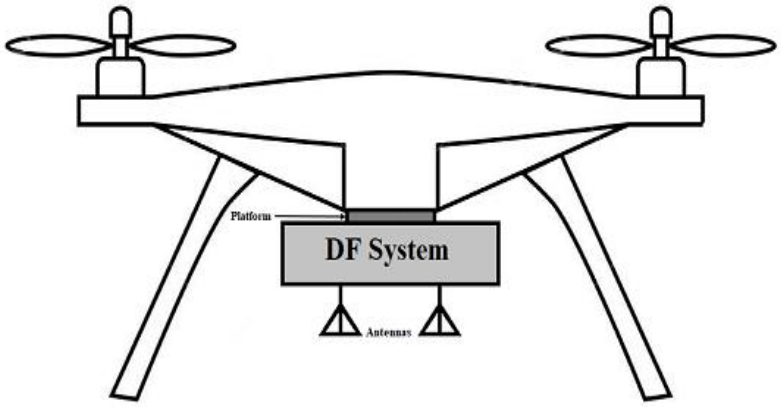

Figure 3.1: System model conceptual structure

The DF system as discussed in section 2.2 consists of DF antenna, RF receiver, and a digital signal processor to calculate the bearing of the transmitter. The system could also be integrated with a display for ground solutions or a communication link for airborne scenarios. More details about the hardware needed to build this DF system will be addressed in Chapter 4. Figure 3.2 shows the components of the DF system.

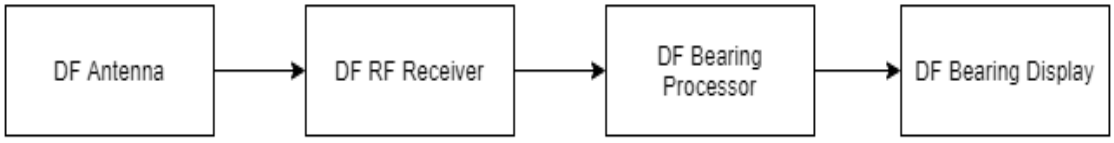

Figure 3.2: DF system components

3.2. Phase-Based Passive DF Approach

In this thesis, the focus will be on the phase-based DF methods such as MUSIC algorithm. The DOA can be estimated by measuring the phase of multiple copies of the received signal that are received by an antenna array.

For long propagation distances, the transmitted RF signal becomes a plane wave. Assume the transmitter emits a single-tone signal of the form

$$s(t) = A\cos(\omega_0 t + \emptyset_{T_x}) \tag{3.1}$$

where A is the signal amplitude, ϕ_{Tx} represents the transmitted signal phase, and ω_0 represent the angular frequency. Figure 3.3 shows a uniform linear array (ULA) antenna structure with two antennas. The signal received at CH2 element is a delayed version of the signal received at CH1 element. The spacing between the two antennas d is known, and the angle θ represents the received angle, which is also known as the direction of arrival (DOA).

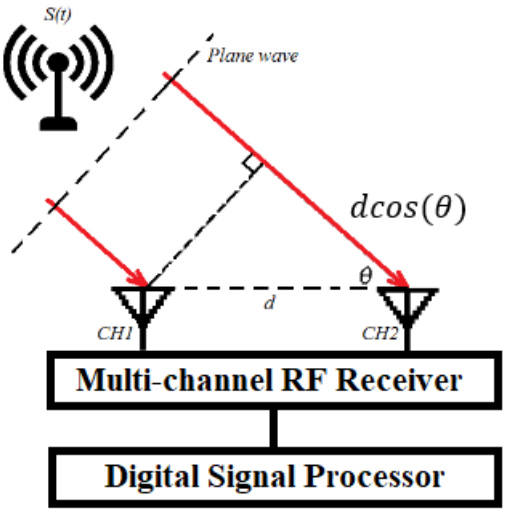

Figure 3.3: Two elements ULA receiver

Assuming CH1 as the reference element, CH1 and CH2 received signals (S_1, S_2) can be expressed as follows:

$$s_1(t) = A\cos(\omega_0(t - T_p) + \phi_{T_x}) \tag{3.2}$$

$$s_2(t) = A\cos(\omega_0(t - T_p - \tau) + \phi_{T_x}) = A\cos(\omega_0(t - T_P) + \phi_{T_x} - \omega_0\tau) \tag{3.3}$$

$$\phi = \omega_0 \tau \tag{3.4}$$

where T_p represents the propagation time delay from the source to CH1 element, τ represents the time delay of the signal to propagate from the wavefront to channel 2, ϕ represents the phase difference between the two signals in radians.

From Figure 3.3, using the known spacing between the antennas *d* and the speed of light *c*, the time delay τ can be calculated as:

$$\tau = \frac{d \cos(\theta)}{c} \tag{3.5}$$

Using Equations (3.5) and (3.6), we can now relate the phase difference ϕ with the DOA θ using the following formula:

$$\theta = \cos^{-1}(\frac{c}{d}\frac{\phi}{\omega_0}) \tag{3.6}$$

Hence, the DOA can be estimated using the phase difference and the knowledge of the received signal frequency. However, this derivation is only valid for this simple case of 2 elements ULA, and it is not to be generalized for other geometries.

3.3. Received Signal Model

As explained in the previous section, received signals phase difference is related to the DOA. A general representation of this phase delay is what is known as the steering vector, which was explained in Section 2.3.4.

The steering vector demonstrates mathematically why an antenna array possesses spatial selectivity. For a ULA antenna array with *K* elements, the steering vector *v(n)* can be calculated as follows:

$$v(\theta) = \begin{bmatrix} 1 \\ e^{-j2\pi\frac{d\sin\theta}{\lambda}} \\ e^{-j2\pi\frac{d\sin\theta}{\lambda}2} \\ . \\ . \\ . \\ e^{-j2\pi\frac{d\sin\theta}{\lambda}(K-1)} \end{bmatrix} \tag{3.7}$$

where *d* is the spacing between the ULA elements, and λ is the wavelength of the signal. The ULA spacing is frequently selected as $d = \lambda/2$, hence the steering vector for ULA can be simplified into:

$$v_m(\theta) = e^{-j\pi \sin\theta\, m}, \;\; m = 0, 1, .., K-1 \tag{3.8}$$

For two degrees of freedom localization, as in azimuth and elevation, ULA is not suitable because it can be used to measure only singular DOA. Other geometries such as uniform circular array (UCA) can be used instead.

The UCA elements are placed on a circumference of a fixed radius, and the spacing between the elements depends on their number [47]. The array steering vector for an *n-th* element array, with wave number $k = 2\pi/\lambda$ can be found using equation (3.10).

$$v(\theta, \phi) = \begin{bmatrix} e^{-j\,2\pi\frac{r}{\lambda}(\sin\phi\ \cos\theta)} \\ e^{-j\,2\pi\frac{r}{\lambda}(\sin\phi\ \cos(\frac{2\pi}{K}-\theta)} \\ . \\ . \\ . \\ e^{-j\,2\pi\frac{r}{\lambda}(\sin\phi\ \cos(\frac{2\pi(K-2)}{K}-\theta)} \\ e^{-j\,2\pi\frac{r}{\lambda}(\sin\phi\ \cos\left(\frac{2\pi(K-1)}{K}-\theta\right)} \end{bmatrix} \tag{3.9}$$

where Θ is the azimuth angle of the DOA, and $\emptyset$ is the elevation angle of the DOA, *K* is the antenna elements number, and *r* is the radial length between the elements and the center of the structural array.

The received signal x_n model can be expressed using the steering vector representation as:

$$x_n = \sum_{p=1}^{K} s_{p,n} v\left(\theta_p, \phi_p\right) + u_n \tag{3.10}$$

where *v* is the steering vector obtained at angle θ_p, u_n is the additive noise received on each antenna element.

3.4. Phase-based Estimation Techniques

IQ demodulation and the DFT techniques presented in Chapter2 are not actually DOA estimation techniques. They are digital signal processing techniques that can be

used to find the phase difference between two signals. However, if the transmitted signals are single-tone (i.e. they are sinusoidal), the DOA can be related directly to the phase between the signals.

3.4.1. IQ demodulation technique. Figure 3.4 shows the steps of IQ demodulation to obtain the phase difference of two received signals s1 and s2.

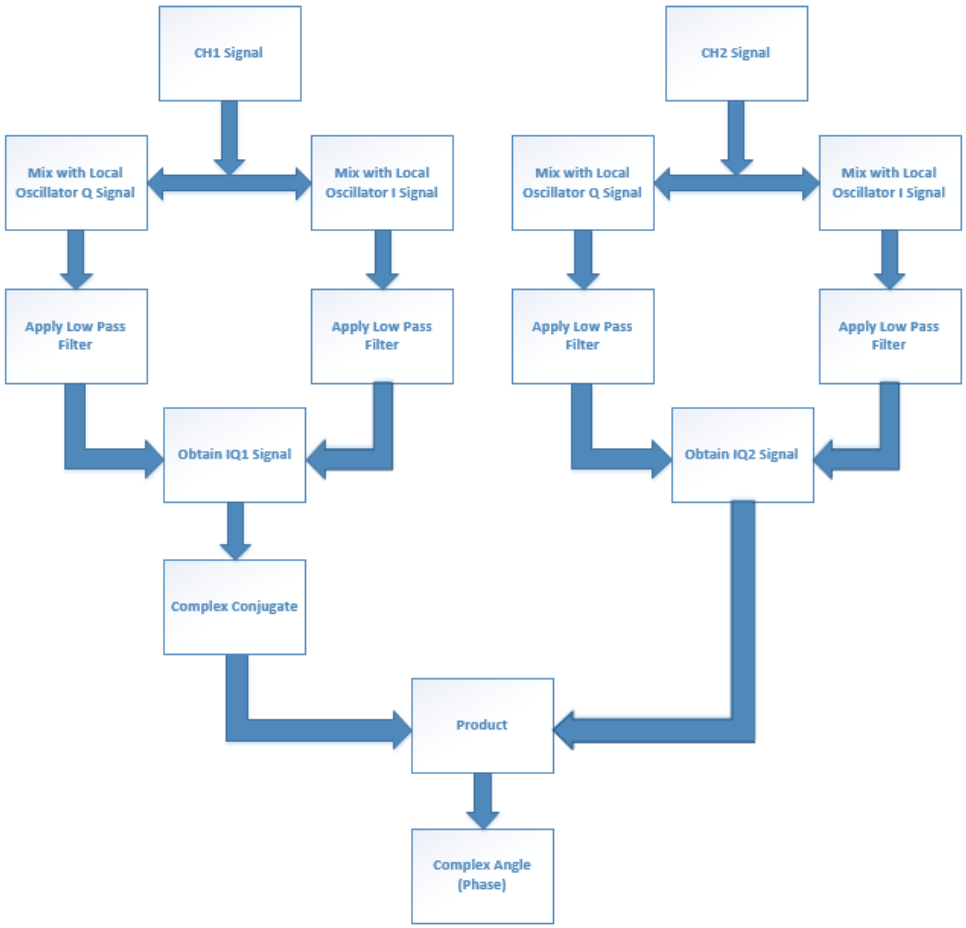

Figure 3.4: IQ demodulation flow chart

3.4.2. DFT technique. If the measured signals are finite in time, the DFT spectrum *X(k)* can be found by sampling the DTFT spectrum X($j\omega$). To obtain the phase difference from the frequency specifications, the DC offset has to be removed from both signals then perform any DFT method such as Fast Fourier Transform (FFT) to obtain the frequency spectrum.

Then by finding the maximum frequency components, the phase difference can be calculated using their corresponding complex angles.

3.5. MUSIC DOA Estimation

To estimate DOA in 2D (i.e. azimuth θ and elevation ϕ), the first step is obtaining the received signal x_n which was presented in equation (3.10). The received signal model will be used as:

$$x_n = \sum_{p=1}^{K} A_p \, s^*_{p,n} v(\theta_p, \phi_p) + u_n(\sigma) \quad (3.11)$$

where θ_p, ϕ_p are the DOA, A_p is the received signal amplitude, σ is the noise level, K is the number of antenna elements in the array. s^* is the imperfect received signal of source p, this imperfection could happen to various hardware and environment anomalies which will be discussed in Section 4.6. The antenna array will be constructed as a uniform circular array that can be affected by hardware anomalies, hence the steering vector will be computed as:

$$v(n) = \exp(-j\frac{2\pi}{\lambda} r_n \cos(\phi_n) \sin(\phi_p) (\cos(\theta_n) \cos(\theta_p) + \sin(\theta_n) \sin(\theta_p)) \quad (3.12)$$

where r_n, θ_n, ϕ_n are the angular positions of the antenna elements.

After obtaining the received signal, the next step is calculating the auto-correlation matrix R_{xx} as explained in equation (2.3). Then, the eigen-decomposition is performed on R_{xx} on to obtain the eigenvectors. Using the rearranged eigenvalues, the number of received signals P can be estimated.

By excluding the signal subspace using the number of received signals P, the MUSIC search algorithm can be applied on the noise subspace. The MUSIC algorithm sweeps the entire range of -90^o to 90^o in azimuth plane and 0^o to 90^o in the elevation plane, to find the spatial spectrum using the equation:

$$f_{MUSIC}(\theta, \phi) = \{ \| v^H (\theta, \phi) E_i \| \}^{-2} \quad (3.13)$$

where E_i is the noise subspace presented in equation (2.5). This search uses the 2D steering vector v for the uniform circular array, which was presented in equation (3.9). The resulting spatial spectrum can be visualized as a heat map where the values closer to the estimated DOAs have high MUSIC values.

A peak finding algorithm was integrated with the MUSIC to automatically locate the peaks in code without the need to be distinguished by the operator. The peak

finding algorithm searches for the peaks in the MUSIC spatial spectrum that are separated by a calibrated factor and have a calibrated threshold value. A general description to the algorithm steps shown in Figure 3.5.

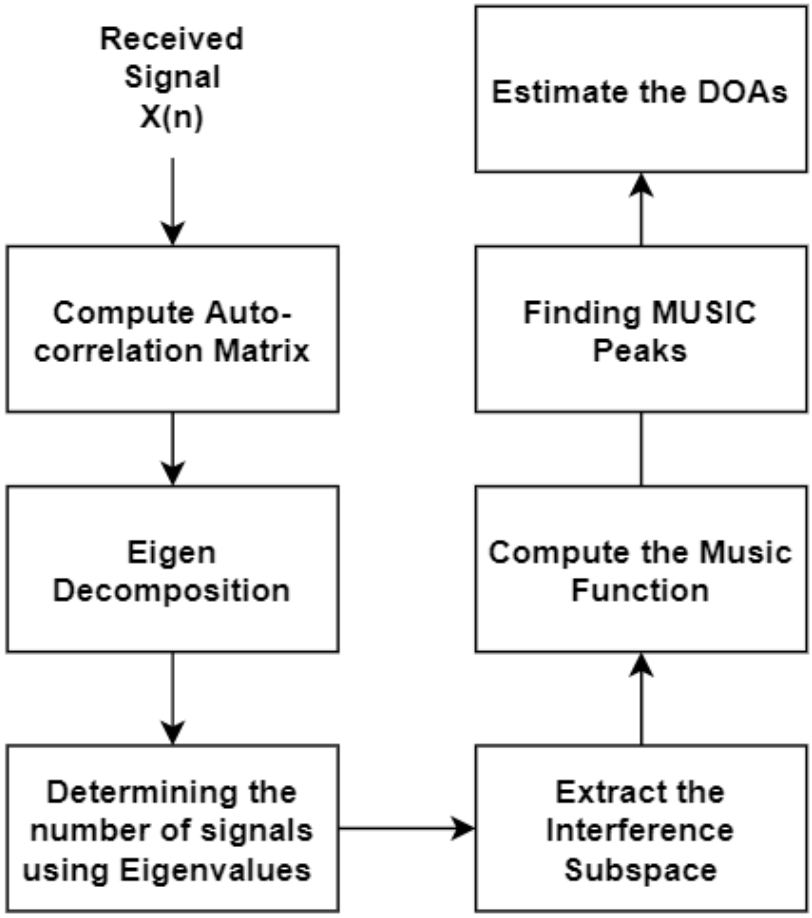

Figure 3.5: MUSIC algorithm

3.6. Geolocation of RF Transmitters

Passive DOA techniques provide only the direction of the transmitters. To achieve source geographical localization, the DOA need to experience set of steps to be converted into valid geographical position. For a DF system mounted on a mobile platform such as UAV, the DOA information is not sufficient without the position of the UAV of when it has sensed that location.

Hence, naturally, the DF system have to be integrated with a navigation system that provides the position and attitude of the carrier platform. Figure 3.6 shows a conceptual block diagram of this integration.

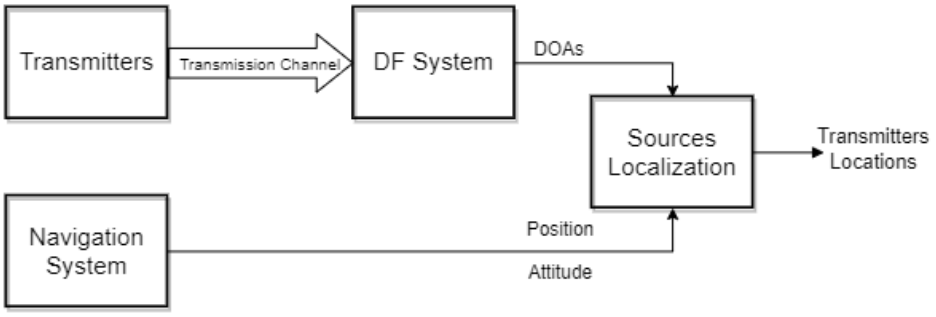

Figure 3.6: Geographical source localization with DF and navigation system

One more method that is used to achieve localization is triangulation by using the information received from different DF systems, with a known position from each other. This technique could be used for drone swarm scenarios.

Figure 3.7 shows the information flow diagram when integrating the DF and navigation systems to achieve geolocation. More details about this in the following sections.

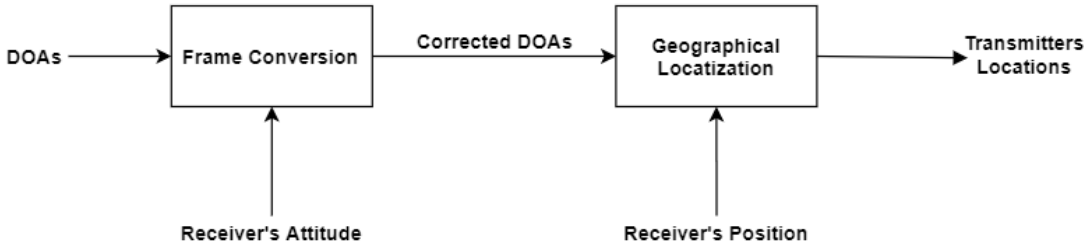

Figure 3.7: Geographical location estimation technique

3.6.1. Frame conversion. For every navigation system, we have to define reference frames to define the positions of interest accurately. There are many reference frames to select from them according to the application and navigation algorithm as mentioned in Section 2.6.

According to this study, body and navigation frames are needed to be used to estimate the transmitters positions. Body frame is the frame which coincide with the body of the flying object, X-axis pointing to the front side of vehicle, Y-axis pointing to the right wing, and Z-axis pointing down. Navigation frame in which all navigation equations are solved, and the rotation of the body frame is transformed with respect to it and then transmitted to the ground station. For our system we can work with NED

(North, East, Down) as a navigation frame, X-axis pointing to north, Y-axis pointing east, and Z-axis pointing down.

A transformation matrix is needed to convert between these two frames in every time step. C_b^n is a transformation matrix from body to navigation frame. It can be defined using the initial position of the body frame with respect to the navigation frame using Equation (3.11):

$$C_p^n = \begin{bmatrix} \cos A \cos r - \sin A \sin p \sin r & -\sin A \cos p & \cos A \sin r + \sin A \sin p \cos r \\ \sin A \cos r + cos A \sin p \sin r & \cos A \cos p & \sin A \sin r - \cos A \sin p \cos r \\ -\cos p \sin r & \sin p & \cos p \cos r \end{bmatrix} \quad (3.11)$$

There are several methods to update the transformation matrix C_b^n: Euler angle method, direction cosine method, and quaternion method. The three Euler angles: pitch p, roll r, and yaw A can be extracted from the transformation matrix as follows:

$$p = \arctan\left(\frac{r_{32}}{\sqrt{r_{12}^2 + r_{22}^2}}\right) \quad (3.12)$$

$$r = \arctan\left(\frac{r_{31}}{r_{33}}\right) \quad (3.13)$$

$$A = \arctan\left(\frac{-r_{12}}{r_{22}}\right) \quad (3.14)$$

3.6.2. Combining DOA with the navigation system. After estimating the DOA, the geographical location of the target can also be approximately estimated using the system current location combined with the DOA. In this section, 3D point to point distance formula based on triangulation will be used in order to estimate the transmitters locations. Because the distances are not larger than line of sight distance, the Earth will be considered as a flat surface to simplify equations.

To make things simpler, the scenario of a single transmitting source will be assumed, as can be seen in Figure 3.8. Assume the DF system carrier platform current location is (X_R, Y_R, Z_R), estimated from the navigation algorithm. The DOA is estimated using MUSIC algorithm to be (θ,ϕ) as in (*azimuth*, *elevation*), and the transmitter location is (X_T, Y_T, Z_T). The distance W is known as the ground distance, whiles, R is the absolute distance or the slant range.

The ground level could be specified by the operator or obtained from a Google map-related algorithm. Let us assume the target altitude Z_T is on the sea level Z_0, the

difference in longitude, latitude, and altitude difference X, Y, and Z, respectively, can be calculated by:

$$X = X_R - X_T \tag{3.15}$$

$$Y = Y_R - Y_T \tag{3.16}$$

$$Z = Z_R - Z_T \tag{3.17}$$

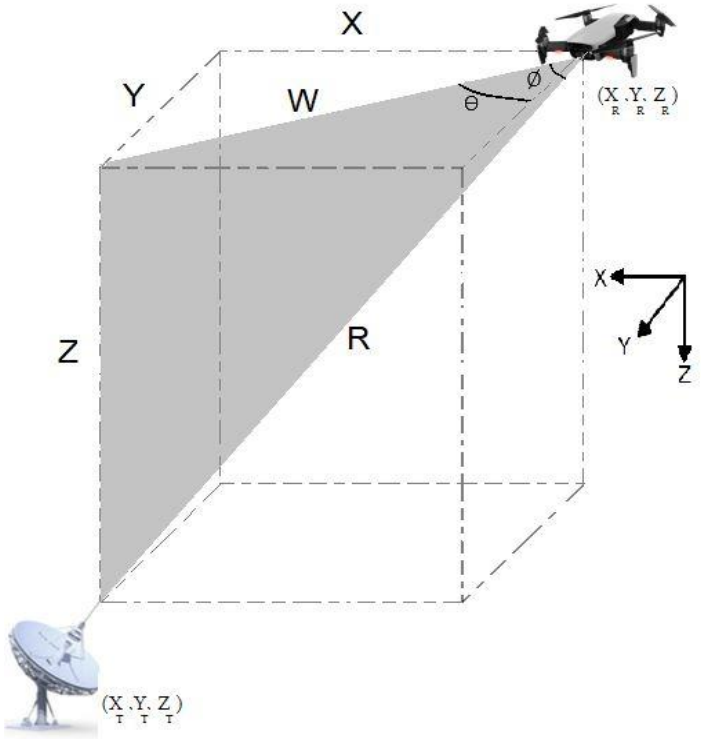

Figure 3.8: Airborne array scenario

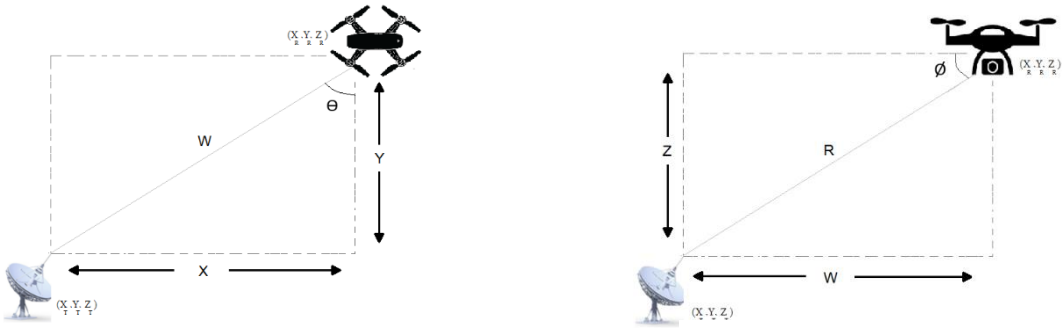

(a) Azimuth view (b) Elevation view

Figure 3.9: Airborne array scenario, 2D views

Then, by using triangulation with the aid of the 2D views shown in Figure 3.9, the ground distance W_T, longitude X_T, and latitude Y_T differences can be calculated using the DOAs, as explained in Equations (3.18 – 3.22).

$$Z = R \sin(\phi) \tag{3.18}$$

$$W = R \cos(\phi) \tag{3.19}$$

$$W = Z \cot(\phi) \tag{3.20}$$

$$X_T = X_R + W \sin(\theta) \tag{3.21}$$

$$Y_T = Y_R + W \cos(\theta) \tag{3.22}$$

Chapter 4. Experimental Setup and Hardware Design

In this chapter, the overall system hardware design, selection, and integration for all components will be addressed. The hardware requirements and components design and selection required to achieve the research objective will be discussed. Furthermore, examples and recommendations of components as well as complete systems solutions will be presented and discussed.

4.1. Hardware Requirements

Based on the thesis objectives, several considerations should be put in mind when designing and implementing the DF system, as well as choosing the platform which it will be installed on. As shown in Figure 3.2 the DF system consists of a DF antenna, DF RF receiver, DF bearing processor, and a DF bearing display. Each component requires distinct specifications based on the application, frequency, system form factor, and the compatibility with other components.

4.1.1. DF antenna requirements. The DF system should contain a receiver with an antenna array to receive multiple copies of the signal, which is needed to perform the array processing for passive direction-finding techniques. The array need to be in a non-linear structure in order to find both azimuth and elevation. One approach that could be suggested is using two orthogonal linear arrays to find both angles, however, this approach is invalid because the DOAs are coupled and the angles cannot be estimated separately.

4.1.2. DF receiver requirements. RF receivers are mostly integrated circuits designed to receive radio frequency signals and converts them from radio waves to electrical signals that can be processed by the digital systems. Generally, the RF receiver contains amplifiers, filters, mixers, local oscillators, demodulators, and analog-to-digital converters (ADC). Some receivers also contain additional features such as data interface, tuning circuits, and other components.

For passive direction-finding, phase difference is the main factor in determining the direction of arrival. For a DF system with an *n*-element antenna array, it should has *n*-received signals. The RF receiver should not alter the phase of the received signals differently or this will lead to incorrect measurements of the DOA. Hence, the DF system must have coherent RF receiving channels, either a single RF receiver or

multiple receivers that are synchronized. To achieve this coherence, some specifications are required when choosing the RF receiver:

- Synchronized local oscillators:

The mixer uses a local oscillator (LO) to down-convert the RF frequency into baseband frequency that can be processed with digital systems. All channels should be mixed with the same LO or a phase-synchronized LOs to maintain the phase difference between all receiving channels.

- Synchronized ADCs:

The ADC converts analog signals into digital by sampling and quantization using a clock source. All receiving channels should have synchronized ADCs that are running using the same clock source.

The selection of the RF receiver depends on the number of its receiving channels (each antenna element requires a separate receiving channel), frequency range of operation, desired bandwidth, form factor, and phase synchronization capabilities.

4.1.3. DF processor requirements. The DF processor is responsible for powering, configuring, and receiving the data from the RF receiver. It can be also used to implement the DOA estimation technique, which requires heavier processing. Each RF receiver can be compatible with a different processor, however, mostly field programmable gate arrays (FPGAs) are used nowadays due to their fast and efficient performance for real-time applications.

4.1.4. System form factor. Form factor for systems refers to the weight, size, and other physical characteristics of the components. For this study, the overall system form factor should be small. The payload should not exceed the maximum allowed on the platform, commercial drones such as DJI UAVs are light-weight with payloads of few kilograms.

4.2. Hardware Array Design

As explained in the requirements above, the system should contain a non-linear antenna array. Some of the non-linear array structure geometries are uniform circular array (UCA), uniform rectangular array (URA), and uniform planar array (UPA). Need to keep in mind that the steering vector $v(n)$ calculations will be different for each

different geometry. The choice of the antenna array geometry mainly depends on the targeted application and the desired antenna beam pattern.

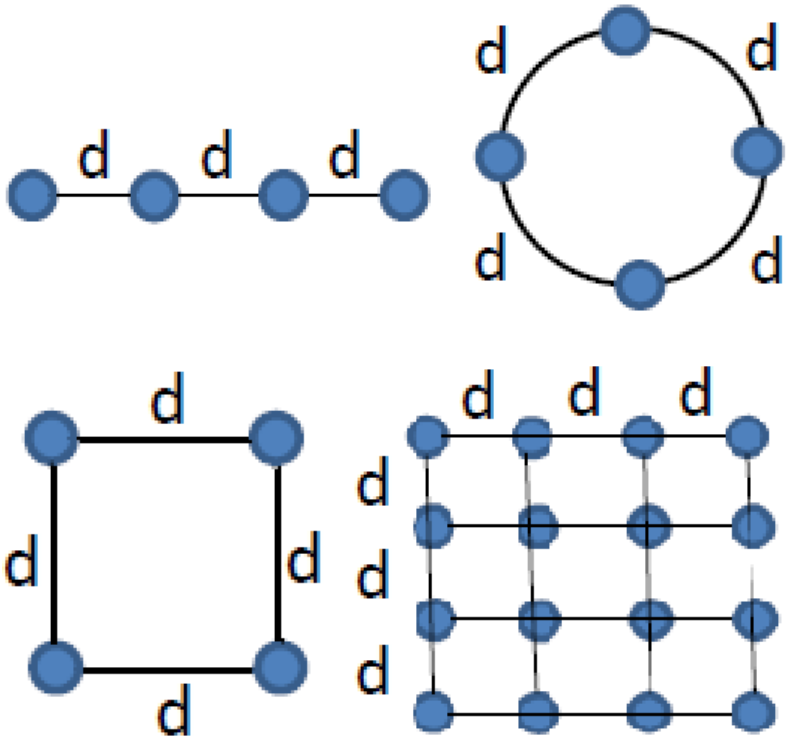

Figure 4.1: Antenna array geometries

Furthermore, the antenna array has to be in a uniform structure, i.e. the elements spacing should be known and fixed for all elements. This spacing is determined by the frequency range of the application. To avoid aliasing, the spacing d should be chosen such that $d < \lambda/2$, where λ is the wavelength of the targeted RF signal. Physical errors in the spacing may affect the antenna performance as well as the coupling between the sensors.

To build the antenna in the geometry needed, the use of RF connectors and cables is inevitable. Usually one cannot connect the antennas directly to the RF receiver since they are not uniformly placed. Typically, RF connectors are used with shielded coaxial cables, in which the shielding is required to lower the reception of electromagnetic radiation from nearby interfering sources and, hence lowering the noise. Those connectors are designed to preserve the shielding that is offered by the coaxial cables design. There are different types of RF connectors shown in Figure 4.2 that differ in their operating frequencies.

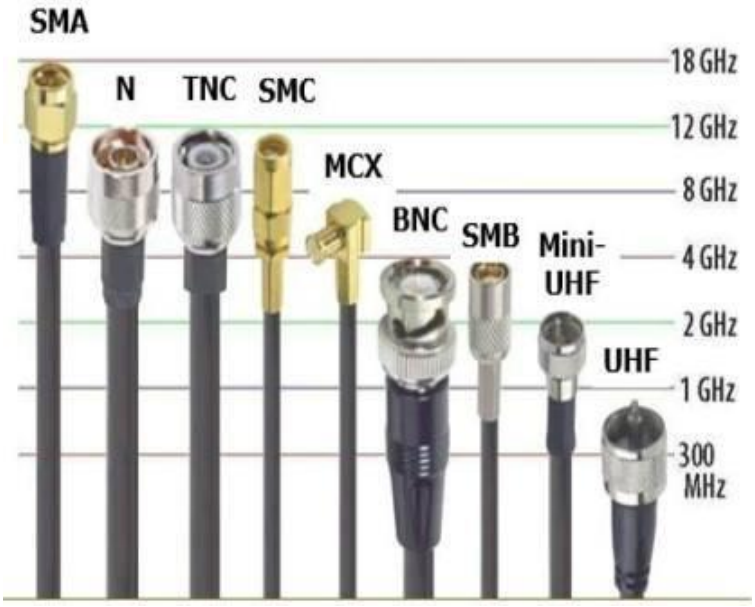

Figure 4.2: Types of RF antenna connectors [48]

4.3. RF Receiver Selection

There are several vendors that offer RF transceivers in the market including Analog Devices Inc. (ADI), Qualcomm Incorporated, STMicroelectronics N.V, Texas Instruments Incorporated, and Silicon Motion Technology Corporation. As discussed in the requirements above, RF receiving channels phase coherence is a main factor in building passive DF systems. Analog Devices produces several highly integrated RF transceivers that offer coherent multi-channel receivers with the ability to synchronize multiple transceivers.

4.3.1. AD9361. The AD9361 chip is a highly integrated RF agile transceiver with high performance, which was designed to be used in 3G and 4G applications. It operates within the frequency range from 70 MHz to 6000 MHz, with adjustable bandwidth from 200 kHz up to 56 MHz. It is ideal for RF applications that require multi-channel transceiver, due to its wideband capability and programmability. As can be seen in Figure 4.3, it contains RF front with flexible mixer alongside frequency synthesizers and that it provides configurable digital interface to the processor [47].

AD9361 provides automatic gain control (AGC) system, which maintains high performance under varying temperature and input signal variations. The receiver includes all necessary blocks to receive RF signals, demodulates them, filters them, and finally digitizes them to be processed afterwards with a Digital Signal Processor (DSP).

The receiver contains two independent channels that can receive two input signals from different sensors, which allows the device to be used in multiple input multiple output (MIMO) systems. It includes a universal frequency synthesizer, which makes it suitable for the intended DF application. Most of the complete solutions which will be presented in Section 4.8 are based on this agile RF transceiver.

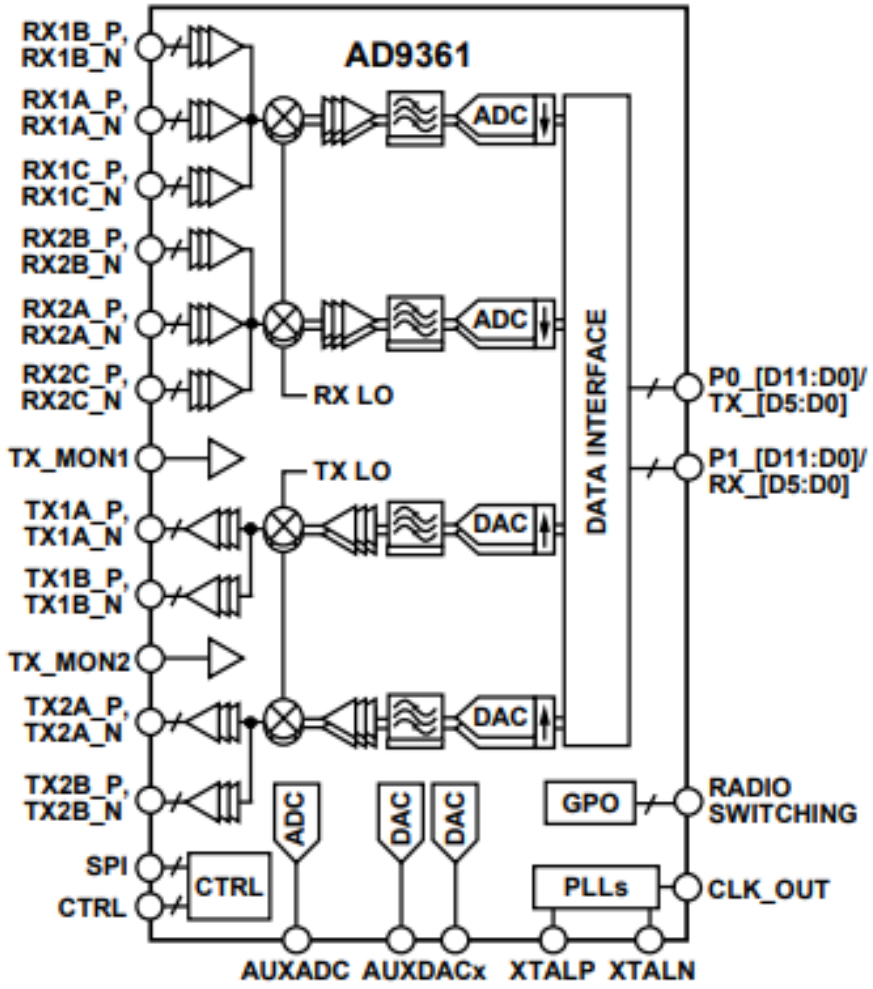

Figure 4.3: AD9361 functional block diagram

The AD-FMCOMMSX-EBZ evaluation and prototyping board belongs to a family of ultra-high-speed analog modules from ADI. It includes an AD9364 (1 Tx, 1 Rx) or AD9361 (2 Tx, 2 Rx) agile RF transceivers and connects them to the Xilinx Field Programmable Gate Array (FPGA) platform. It is fully configurable by software, without the need of any hardware modifications [49]. These rapid development and prototyping boards include AD-FMCOMMS5-EBZ, AD-FMCOMMS4-EBZ, AD-FMCOMMS3-EBZ and AD-FMCOMMS2-EBZ.

AD-FMCOMMS5-EBZ shown in Figure 4.4 integrates dual AD9361 chips, creating a 4x4 MIMO platform [51]. It is powered and configured by dual FMC connectors, which allows it to be integrated with Xilinx ZC706 platform. It provides phase and frequency synchronization for all channels. The dual AD9361 chips are calibrated by using dual ADG918 switches and an API software to create a calibration matrix to achieve full synchronization. Furthermore, it allows the use of external LO signal, which makes it a perfect RF receiver for passive DF application.

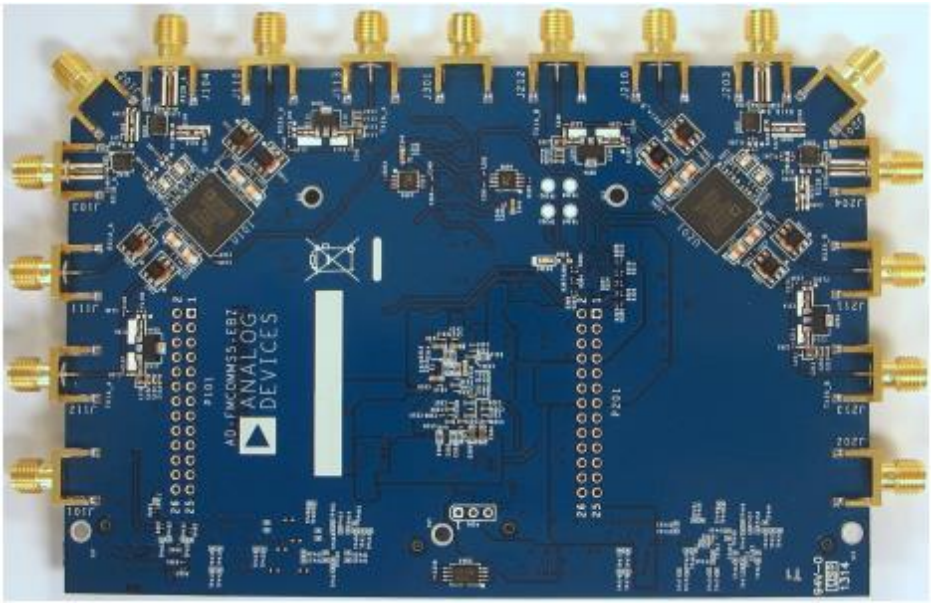

Figure 4.4: AD-FMCOMMS5-EBZ 4x4 MIMO evaluation board

4.3.2. AD9371. The AD9371 transceiver contains dual-channel transmitter and receiver with integrated common local oscillator, RF synthesizers, filters, and DSP functions. It operates within the frequency range from 300 MHz to 6000 MHz, covering most of the cellular bands. The AD9371 integrates all necessary blocks required to achieve transmission and reception using a single chip. The AD9371 receiver consists of two channels, with I & Q mixers connected to the common local oscillator to down-convert the received signal from the passband to the baseband for DSP operations [52].

The ADRV9371 board shown in Figure 4.5 is a software-defined radio (SDR) card designed to demonstrate the potentials of the AD9371 radio transceiver. It presents a single 2x2 transceiver platform, with all peripherals needed for radio operations. Since

to the moment of writing this document, there is no 4x4 MIMO evaluation board for the AD9371 chip, which makes it not suitable for the objective of this thesis.

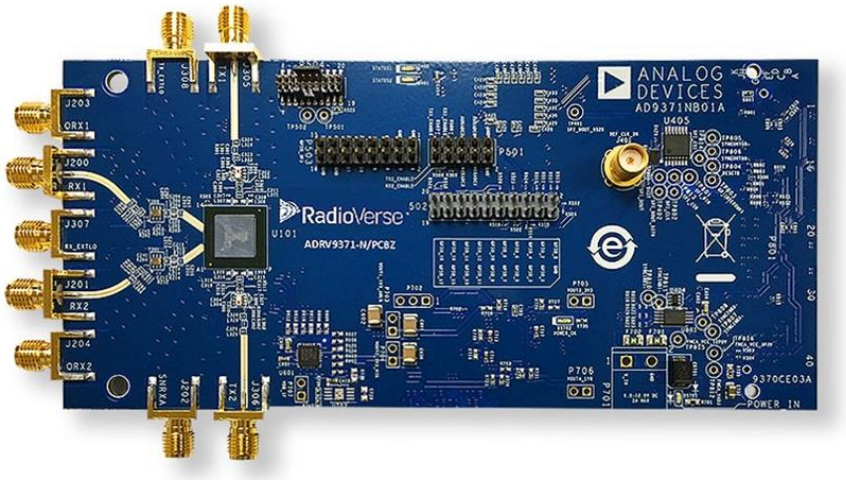

Figure 4.5: ADRV9371 2x2 MIMO evaluation board

4.4. DF Receiver Selection

The selected RF receiver generally decides the choice of the DF processor, since most of the RF receiver have only few compatible carrier platforms processors needed to interface, program, and configure them. When using AD9361 boards, you need a carrier platform such as an FPGA board. The boards recommended by ADI are ZedBoard, Xilinx ZC706, or Arrow SoCKit.

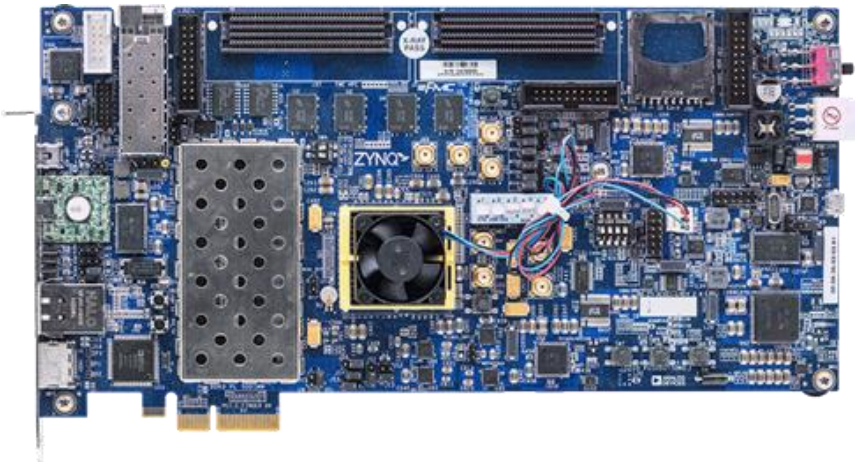

Figure 4.6: EVAL-TPG-ZYNQ3 evaluation board

The AD-FMCOMS5-EBZ uses dual FMC connectors, which means it requires a carrier board with two adjacent connectors. It can be integrated with most of the Xilinx Zynq-7000 evaluation kits such as ZC702 and ZC706. Figure 4.6 shows EVAL-TPG-

ZYNQ3 evaluation kit which is provided from Analog Devices to support RF transceivers with single or dual FMC connectors.

4.5. Overall System Setup

Figure 4.7 shows the DF system constructed using a four-element UCA antenna array of AD-FMCOMMS5-EBZ and Xilinx ZC706 evaluation board. The antenna array is connected using RF connectors and cables to the RF receiver. The FMCOMM board is connected to the FPGA through the dual FMC connectors, which allows the FPGA to power and configure FMCOMM board as well as perform transmitting and receiving operations.

The FPGA can also be used to implement the DOA estimation techniques, or connected through JTAG cables to an embedded-PC in which the algorithm is running.

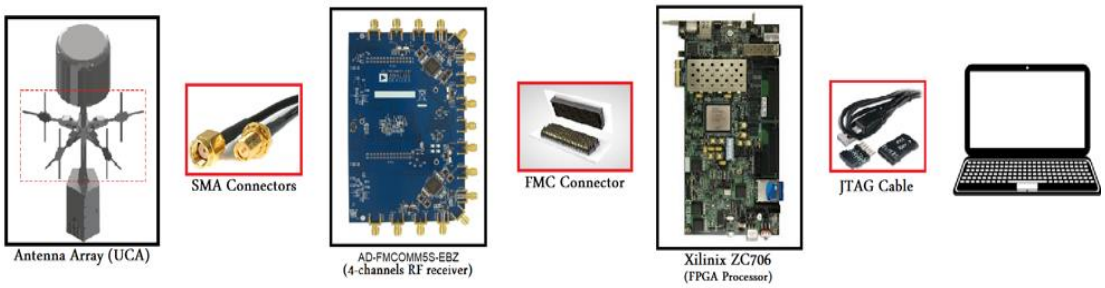

Figure 4.7: DF system hardware setup components

4.6. Realistic Hardware Anomalies

The goal of this study is to design and simulate a realistic direction finding and localizing system using airborne antenna array, however, there were some assumptions in the previous sections that could be invalid when actually building the hardware of the system. In this section these hardware anomalies will be analyzed and discussed.

4.6.1. Non-uniform antenna array. For 3D localization (i.e. 2D MUSIC DF finding), we need to use a non-linear antenna array to estimate both azimuth and elevation, as discussed in Section 3.3. For this study, uniform circular array will be used. For a UCA, the antenna elements should have fixed spacing and should all be on the same plane. Figure4.8 shows the uniform structure of a circular array.

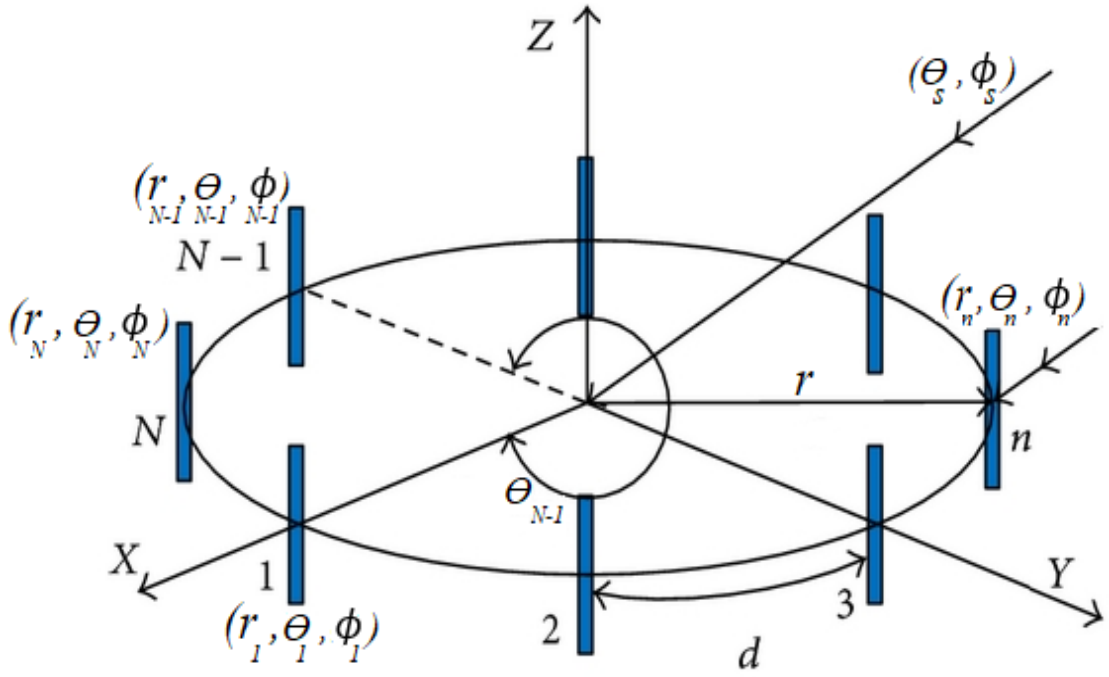

Figure 4.8: Uniform circular array in 3D environment

Where r is the radius of the circular structure. d is the spacing between successive sensors. The spacing and the number of elements decide the radius of the structure. Θ_S, ϕ_S are the DOAs of the received signal (azimuth and elevation). r_n, Θ_n, ϕ_n are the spherical coordinates of the antenna element n w.r.t. the center of the circular structure.

In the uniform structure, the radial distance r_n is equal for all array elements, because all elements are at equal distances from each other. For a horizontally polarized antenna, ϕ_n will be zero so all elements are in the horizontal planar (xy planar). Following these assumptions, the steering vector $v(n)$ for a uniform circular array (UCA) with K elements can be simplified as follows:

$$r(n) = r\,, \qquad i = 0, 1, 2, \dots, K-1 \tag{4.1}$$

$$x(n) = r\cos(\theta_n) \tag{4.2}$$

$$y(n) = r\sin(\theta_n) \tag{4.3}$$

$$v(n) = \exp(-j\frac{2\pi}{\lambda}\sin(\phi_S)\left(x(n)\cos(\theta_S) + y(n)\sin(\theta_S)\right) \tag{4.4}$$

For a non-uniform circular array, this simplification is invalid. The formula has to be extended to accommodate for antenna displacements and irregularities. For an antenna element as position (x, y, z), the steering vector will be derived as follows:

$$v(n) = \exp(-j\frac{2\pi}{\lambda} r_n \cos(\phi_n)\sin(\phi_S)\,(\cos(\theta_n)\cos(\theta_S) + \sin(\theta_n)\sin(\theta_S)\,) \quad (4.5)$$

The irregularity could be caused by errors in the design, implementation, or other physical hardware anomalies, and they will lead to deviations in the antenna array manifold, hence, resulting in errors in the DOA estimation. These anomalies could be sensors angular displacement, radial (planar) displacement, vertical displacement, or any random undesired deviations in the position of any array element as can be seen in Figure 4.9.

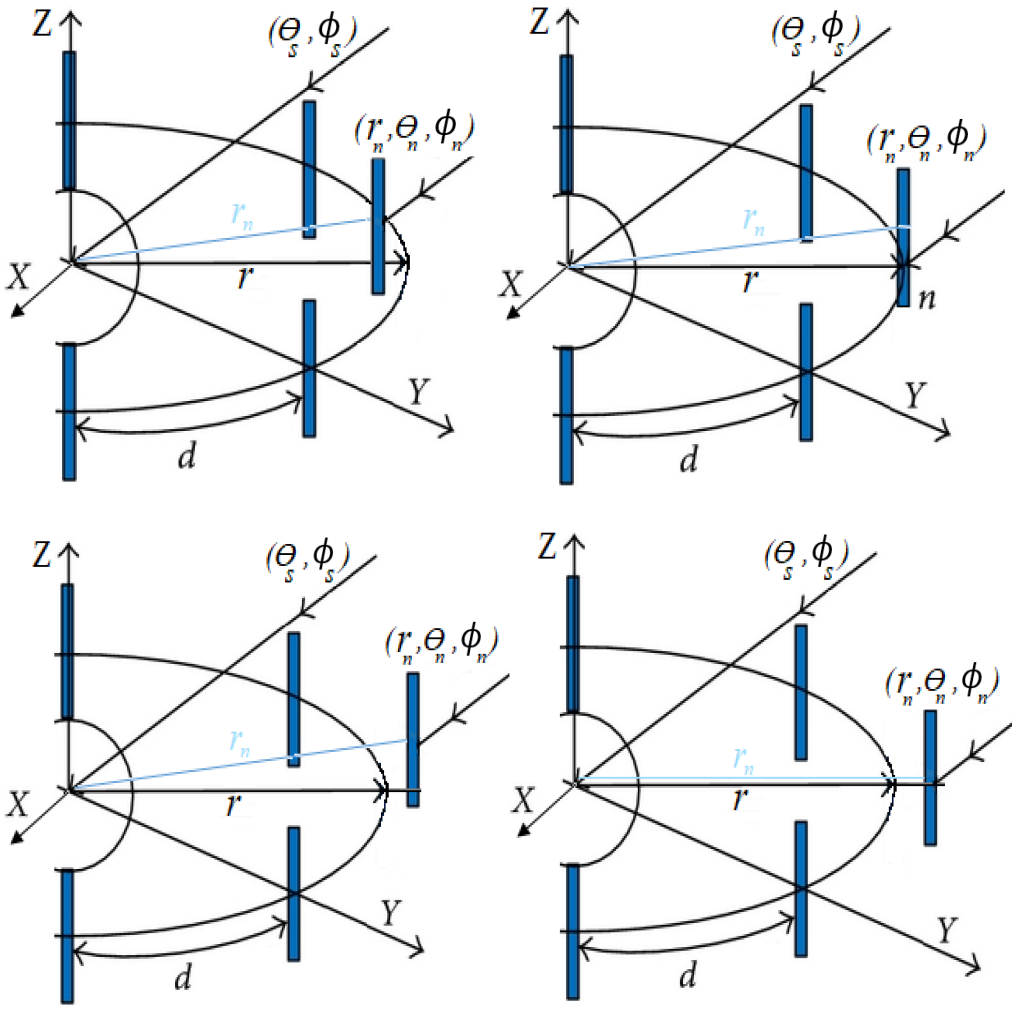

Figure 4.9: Circular antenna array anomalies

4.6.2. Imperfect RF receiver. There are several factors that needed to be considered when designing and building an RF receiver. This includes automatic gain tuning, phase synchronization, DC offset correction, digital filtering, and quadrature correction. The AD9361 receiver eliminates the need for these processes in the digital baseband processing. Nonetheless, some of these anomalies will be discussed and presented in the results.

4.7. Hardware Calibration

The DF system should be calibrated in the laboratory before assembling and mounting on the drone. This calibration mainly includes antenna array calibration as well as phase synchronization between the RF receiving channels, to ensure channels coherence, which is a main factor in passive DF applications .

To compensate for the antenna array anomalies, the array should be calibrated before deploying to the mission to be as close to the uniform structure as possible. For the RF receiver, all the channels should be synchronized using the same local oscillator and the same ADC clock source. The phase deviations could be removed using a known source with a known DOA to calibrate the antenna array on the ground. However, one test that can be done is to eliminate the RF side by connecting the transmitter directly to the receiver. With the proper shielded cables and connectors, the RF current will not be radiated and emitted.

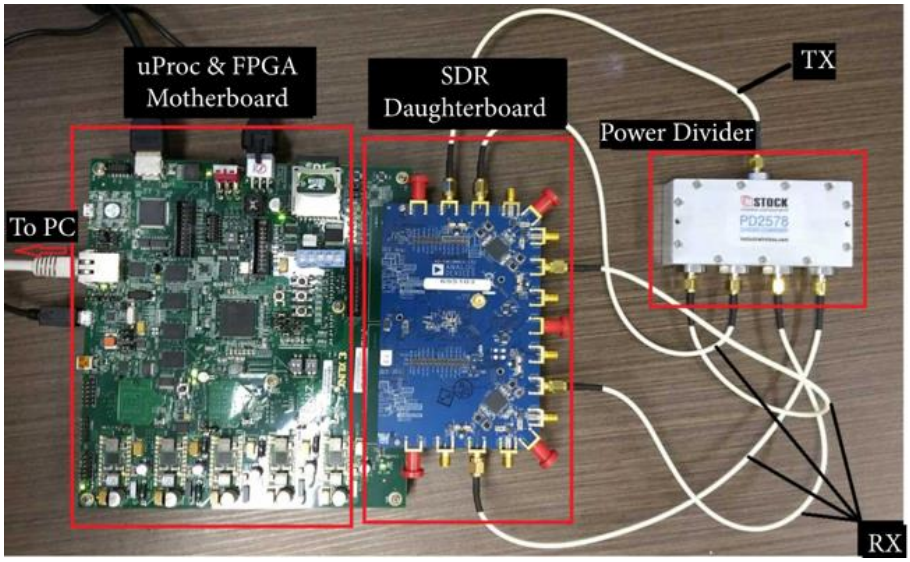

Figure 4.10: Assembled DF system hardware for channels calibration [53]

Figure 4.10 shows a channels synchronization test using AD-FMCOMM5-EBZ connected to a Xilinx ZC702 FPGA. The transmitter signal power is divided into four channels using a phase-coherent power divider, the four receivers of the ADFMCOMM board should receive exactly the same signal with the same phase for a phase-coherent receiver. A novel model to synchronize and calibrate this receiver was published in June 2019 [51].

4.8. Integrated Solutions

Currently, some existing solutions that are suitable for DF applications are availble. Most of them are still in the development stages. Some are open-source to help and encourage developers and engineers to refine, develop, and integrate their solutions into them. However, their validity for airborne solutions are questionable due to their frequency range, efficiency and form factor.

4.8.1. Ancortek 2400T2R4 SDR. Ancortek Inc. is specialized in developing low-power compact SDR development kits operating in different frequency bands. One of their product is the SDR-KIT 2400T2R4 [54], which operates in the K-band 24-26 GHz with 0-2000 MHz. It is designed to support DOA applications with its 4x coherent receiver channels. It also comes as an embedded version with low small factor, which makes it perfect for airborne solutions. Figure 4.11 shows the SDR kit as well as the embedded version of the 2400T2R4.

Figure 4.11: Ancortek 2400T2R4 SDR

4.8.2. KerberosSDR RTL-SDR. KerberosSDR is a 4x phase coherent receiving channels SDR developed by RTL by combining two RTL-SDRs that share a

common clock source, integrated with a noise source to enable syncing both SDRs. Figure 4.12 shows the Kerberos SDR integrated system [55].

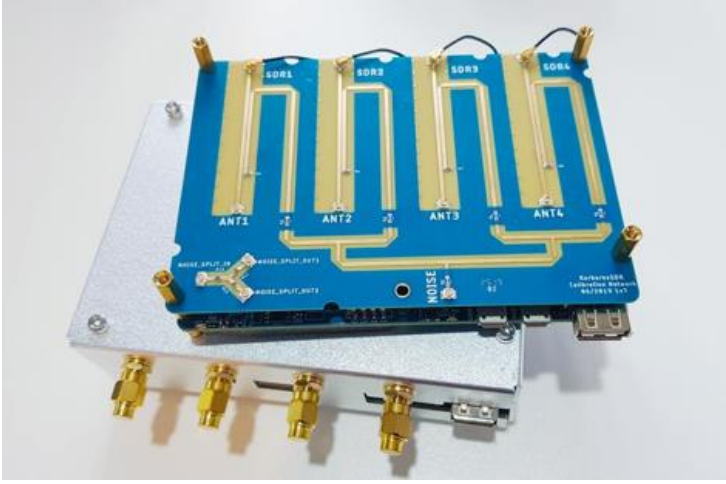

Figure 4.12: KerberosSDR - 4 coherent channels RF receiver

KerberosSDR is in its first version and still an experimental product under development. It has open source that can be extended by the developers. Its operating range is 24 MHz - 1.7 GHz, and usually used in cars navigation, the DOA estimation accuracy is fair, however, the update rate as well as the low frequency range makes it questionable for airborne solutions.

4.8.3. Nutaq Pico SDR. Nutaq provides advanced DSP and technology solutions, including SDRs that supports GNU radio, MATLAB, and Simulink. Nutaq offers PicoSDR that comes in a 4x4 and 8x8 phase coherent channels SDRs, which are designed to support direction finding, phased array, and beam forming applications. Figure 4.13 shows the two SDR options provided by the company.

Figure 4.13: Nutaq Pico SDRs

Chapter 5. Simulation and Results

In this Chapter, the results of the DF estimation techniques and localization will be presented with the aid of the appropriate simulated graphs. The performance of the system in a realistic environment, which was described in Chapter 4, will be evaluated under various testing scenarios, and the results will be demonstrated and subjected to discussion.

The case study assumes the transmitting RF signal is at a far-sufficient distance that is enough to approximately assume that the wavefront is planar. The sampling frequency is taken as *Fs = 8 kHz*, the received signal frequency in its baseband is set as *Fm = 100 Hz* with 1000 samples of the signal per test.

In order to investigate effects of noise on measurements, the signal-to-noise ratio SNR will be varied. Also, antenna array characteristics, RF receiver performance, as well as the number and locations of the transmitting sources will be varied, and the DF system performance is observed, examined, and presented. All the tests are carried out using (R) Core i5 machine @ 2.40 GHz with 8GB RAM and Windows 10 Home 64-bit operating system.

5.1. Phase Difference Estimation Algorithms

As discussed in Chapter 2, passive direction finding is achieved through measuring the phase differences of multiple copies of the received RF signal. Hence, for a receiver with *n* Rx channels, all of these channels should have the same phase in order to achieve a proper DOA estimation. Hardware components of the receiving channels i.e. filters, mixers, as well as non-synchronized sampling may affect the measured phase differences between the RF channels.

Using phase difference measurement techniques, the non-coherent RF channels can be synchronized as has been discussed in Section 4.7 of Chapter 4. Here, in this section, some of the phase difference measurement techniques will be simulated and evaluated.

5.1.1. IQ demodulation. Inphase-quadrature demodulation technique can be used to estimate the phase of signals. Figure 5.1 below shows the Simulink functional

block diagram for the IQ algorithm discussed that has been discussed in Section 2.4.6 of Chapter 2.

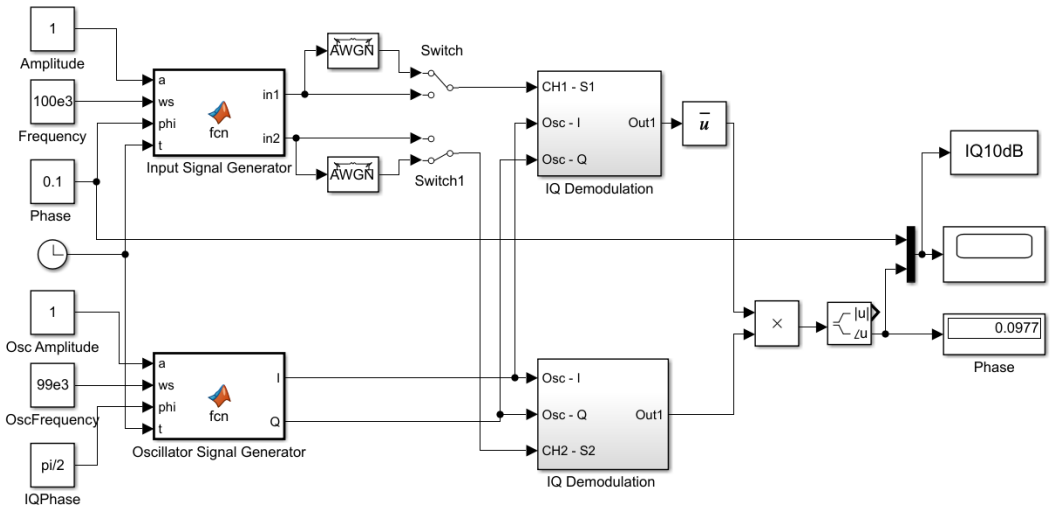

Figure 5.1: IQ demodulation block diagram

Effects of multiple phase differences and different noise levels were tested on the system model. Figure 5.2 shows the results for phase difference estimation of two input signals received with frequency of *100 kHz* and a phase difference of *0.1* radians. The results are accurate, however, for a low SNR values such as *2dB*, the performance rapidly degrades.

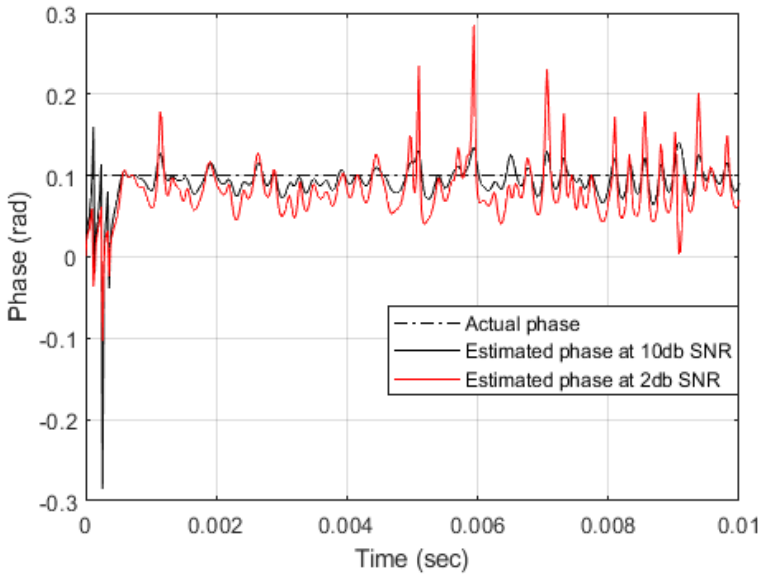

Figure 5.2: IQ demodulation phase estimation results

5.1.2. DFT technique. As shown in Figure 5.3 below, the depicted Simulink functional diagram is used to simulate the DFT method that was discussed in section 2.4.7 of Chapter 2.

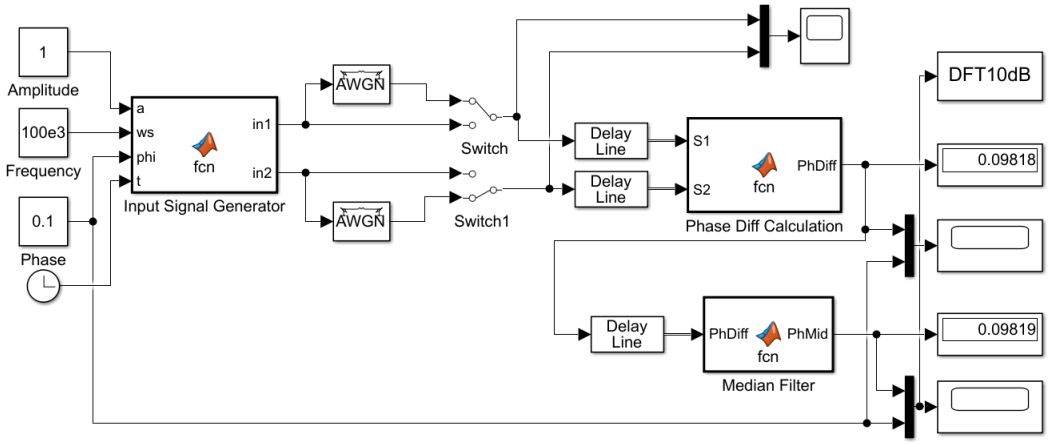

Figure 5.3: DFT technique block diagram

Figure 5.4 shows the results for phase difference estimation of two input signals received with frequency of *100 kHz* and a phase difference of *0.1* radians.

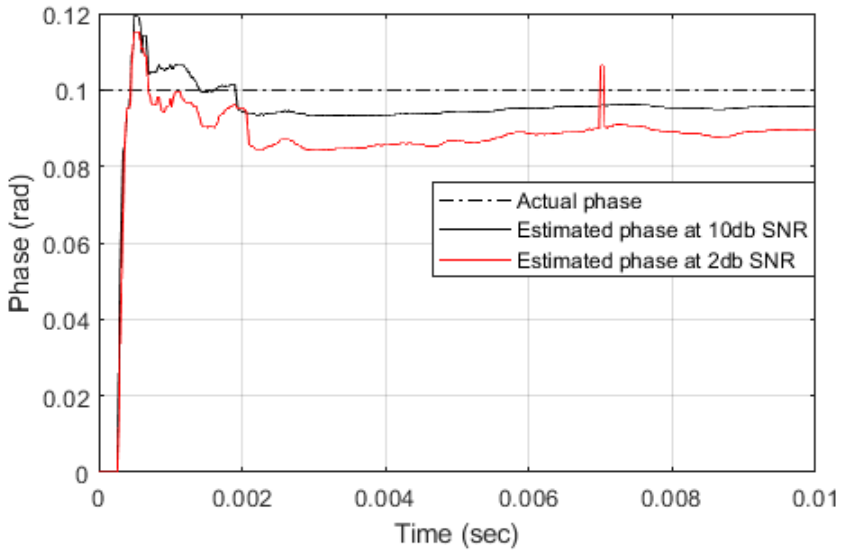

Figure 5.4: DFT phase estimation results

5.2. MUSIC 2D DOA Estimation

This section presents the results for simulation of the MUSIC DOA estimation technique for the measurement of azimuth and elevation (also will be referred to as θ

and ϕ respectively from here onwards). All the results were achieved by processing 1000 time-samples of the received signal. The number of transmitting sources, SNR, and antenna elements number are varied to test the performance of the MUSIC method in different scenarios.

5.2.1. Localizing a single source. Figures 5.5 and 5.6 show the MUSIC DOA estimation simulation results for a single transmitting source at azimuth angle 70^o and elevation angle 20^o. The receiver is designed as a 4-element UCA antenna. The results are exact with *10dB* SNR. For the second scenario, the noise power is increased by setting SNR to *0.5dB*, and the results were fairly accurate with a small deviation. The estimated locations are (θ, ϕ) are found to be *(68.1818 , 20.9091)*.

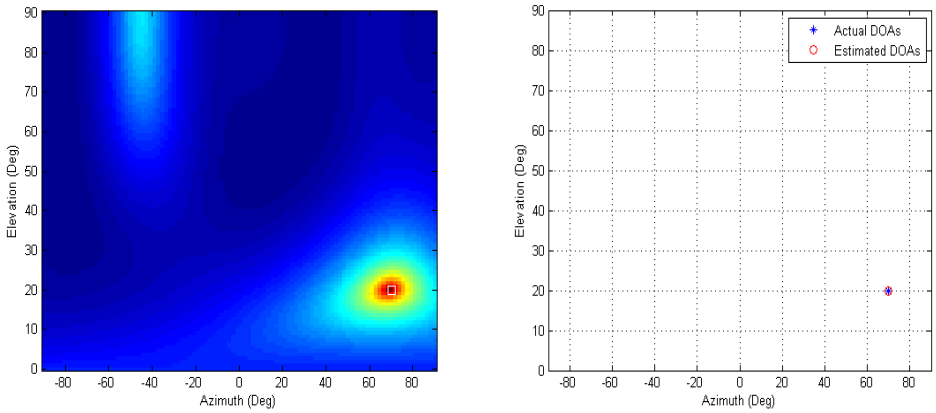

Figure 5.5: MUSIC DOA estimation for a single source with 10 dB SNR

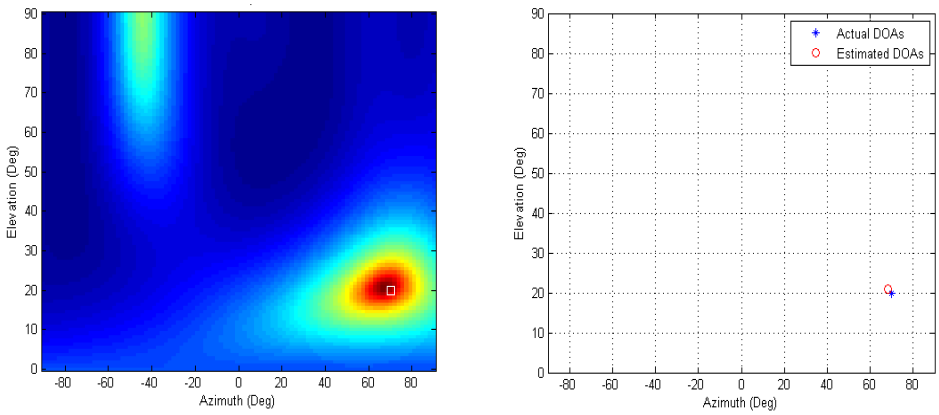

Figure 5.6: MUSIC DOA estimation for a single source with 0.5 dB SNR

MUSIC was tested in wide range of SNR values, and the results are shown in Figure 5.7. The performance of the technique is highly accurate for SNR above *10dB*.

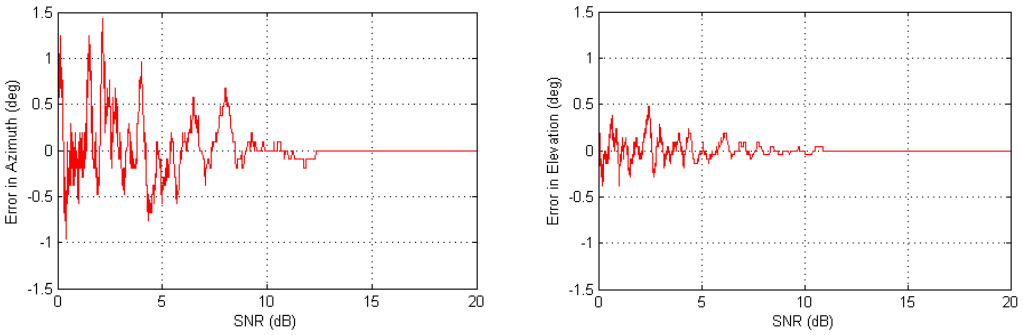

Figure 5.7: MUSIC DOA estimation error for a single source with varying SNR

5.2.2. Localizing multiple sources. As mentioned in section 2.4.2 of Chapter 2, MUSIC algorithm has high-resolution and is able to distinguish between multiple transmitting sources.

Below are the results for the simulation of the DOA estimation of three sources, using 16 elements UCA at different noise levels. Scenario 1 in Figure 5.8 shows the DOA estimation at SNR = *10dB*, while Scenario 2 in Figure 5.9 shows the DOA estimation at SNR = *1dB*.

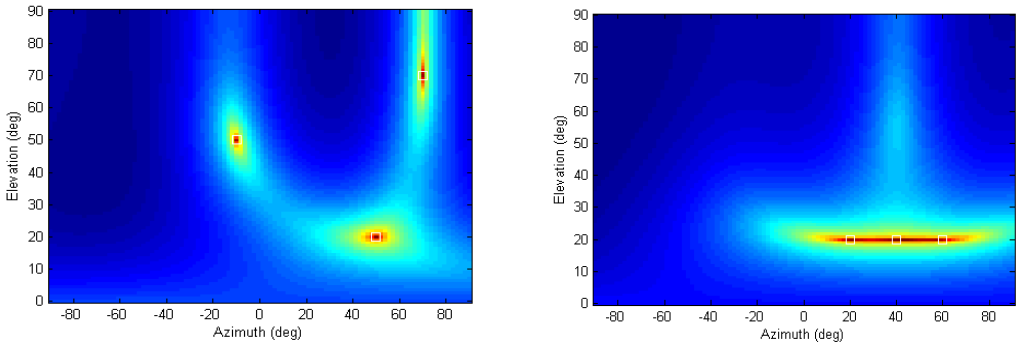

Figure 5.8: MUSIC DOA estimation for multiple sources, Scenario 1

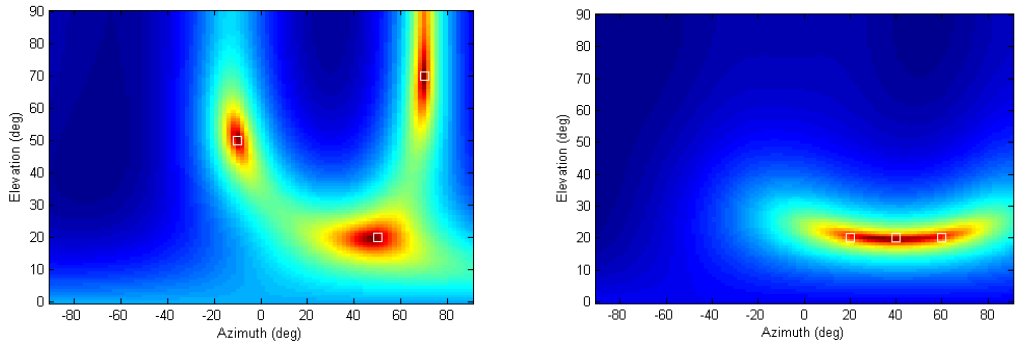

Figure 5.9: MUSIC DOA estimation for multiple sources, Scenario 2

For UAV solutions, MUSIC requires a peak-finding algorithm to automatically find the peaks values. It is inconvienet to store the high complex spectrum of the MUSIC in an embedded system with limited storing capabilites. The performance of the MUSIC peak finder algorithm for the two scearios above is highly accurate.

However, for very close sources to each other, the peak-finder algoirthm might fail to distinguish between the DOAs, specially in high noise scenarios. In Figure 5.10, two sources were very close to each other, wher the has algorithm failed to distinguish between them.

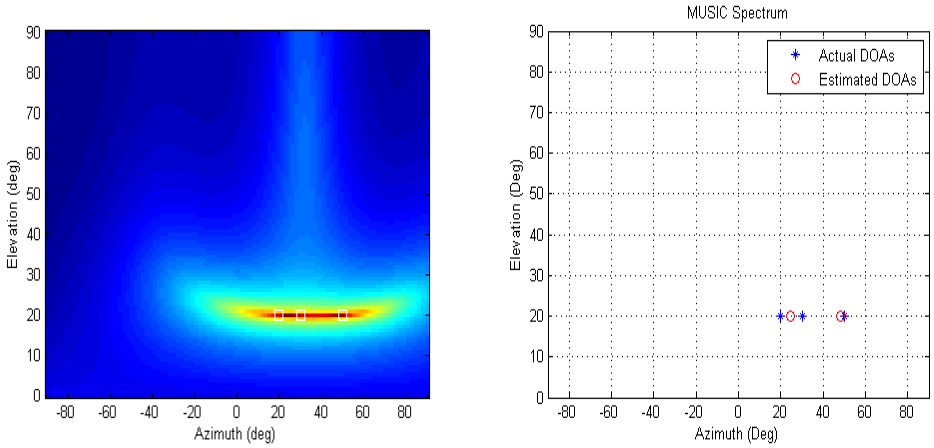

Figure 5.10: MUSIC DOA estimation for multiple sources, Scenario 3

5.2.3. MUSIC MSE. MUSIC 2D DOA estimation was evaluated for a wide range of azimuth and elevation values in different SNR values to test its accuracy. Table 5.1 shows the mean square error (MSE) results for these scenarios.

Table 5.1: MSE in MUSIC DOA estimation accuracy for different ranges and different SNR values

Azimuth Range	Elevation Range	SNR	Azimuth MSE	Elevation MSE
-90^o to 90^o	0^o to 90^o	20 *dB*	78.1456	0.1316
-90^o to 90^o	0^o to 90^o	3 *dB*	252.5650	2.7742
-80^o to 80^o	10^o to 80^o	20 *dB*	0.2912	0.0817
-80^o to 80^o	10^o to 80^o	3 *dB*	1.4142	1.2520
-45^o to 45^o	20^o to 70^o	20 *dB*	0.2827	0.0789
-45^o to 45^o	20^o to 70^o	3 *dB*	1.0196	0.7538

As can be noticed, the MUSIC performance degrades when searching for sources close to the limits of the search spectrum, espically in the azimuth plane. Usually DF systems are designed with limited ranges depending on the application.

5.3. Effect of the Number of Array Elements on MUSIC Estimation

The performance of DOA estimation can be improved by using more antenna array elements. Figure 5.11 shows the MUSIC DOA estimation results for very low SNR values, and compares the DOA for 4 and 16 elements UCA antenna.

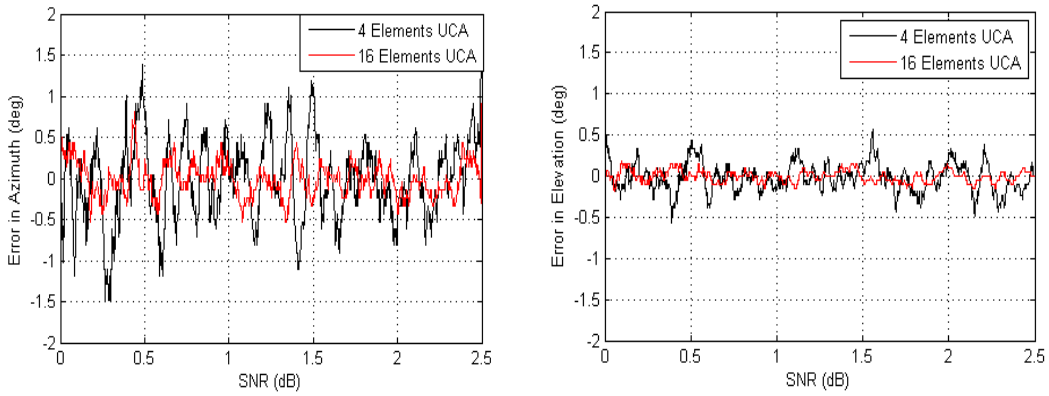

Figure 5.11: MUSIC DOA estimation error for different antenna elements number

It is clear that 16 elements antenna array performance is much better. However, increasing the number of array elements will increase the system cost, weight, and complexity.

5.4. Hardware Anomalies Effect on MUSIC Estimation

In this section, the effects of hardware anomalies in the DOA estimation that were discussed in Section 4.6, will be simulated and their results will be presented.

5.4.1. Antenna displacement anomalies. This section presents the results for the effect of antenna array anomalies in DOA estimation discussed in Section 4.6. For this experiment, the DF antenna is designed as four elements circular array. The position of each of the four array elements is varied by a random displacement in the three axes (*x*, *y*, *z*), using a random displacement with zero mean and the same standard deviation for the three axes.

The algorithm was tested using different standard deviations for the displacement up to *1* cm, and the resulting positions of the array elements *(dx, dy, xz)* are displayed in Figure 5.12 below.

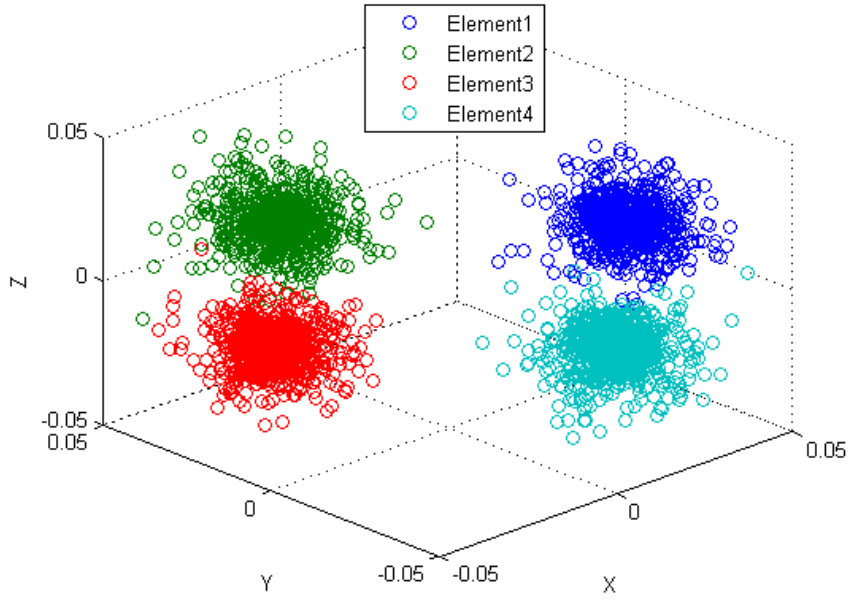

Figure 5.12: Antenna elements displacement in 3D space.

For MUSIC estimation, the received signals were modeled using an imperfect steering vector V_{imp} which was derived in Section 4.6.2. For MUSIC algorithm, the steering vector was assumed for a perfect uniform circular array. Figure 5.13 shows the results for DOA estimation and deviation due to the antenna displacement. The transmitting source DOA was at $(\theta, \phi) = (70^o, 20^o)$, and the SNR was *10dB*.

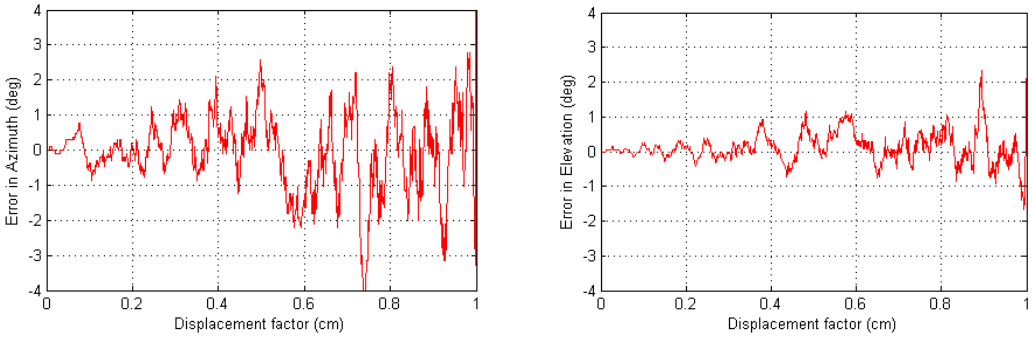

Figure 5.13: MUSIC DOA estimation error for array displacement anomalies

5.4.2. Phase perturbation anomalies. Phase perturbation can happen due to several reasons, including cable heating, cable length and impedance mismatch as well as incoherent RF receiving channels that was as discussed in Section 4.6. Phase perturbation can be one of the biggest challenges to passive direction finding, since it mainly uses the phase difference to estimate DOA. In this section, effects of misalignment phase on the received signals will be presented.

Figure 5.14 shows the received signals amplitude and phase when receiving a signal from DOA $(\theta, \phi) = (0^o, 30^o)$. The receiver consists of a 4-element UCA, and a synchronized RF receiver without anomalies. The SNR is set to *100dB* to clearly show the received signals. Rx1 is the received signal from the reference antenna element.

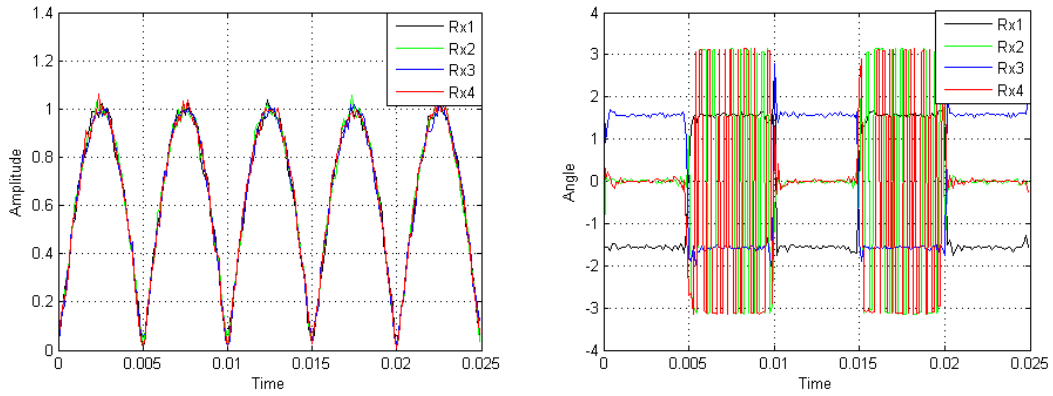

Figure 5.14: Received signals using a synchronized phase-coherent receiver

Scenario 1 shown in Figure 5.15 presents the received signals measurement obtained from assuming the first channel is affected by fixed phase delay. This could be a result of different cable length, non-synchronized local oscillator, or delayed sampling sequence. Figure 5.16 shows the resulting DOA estimation for this scenario

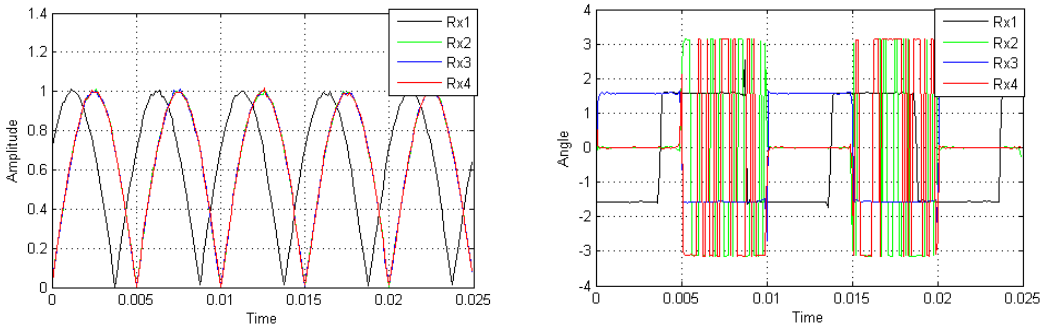

Figure 5.15: Received signals using a non-synchronized receiver, scenario 1

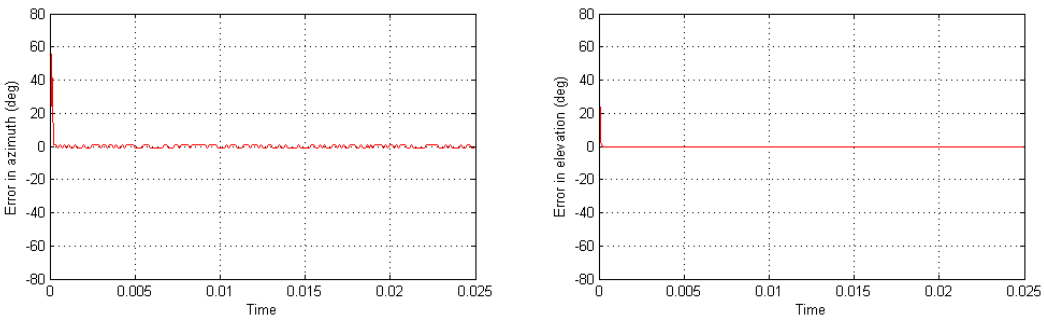

Figure 5.16: MUSIC DOA estimation error for phase perturbation, Scenario 1

Scenario 2 shown in Figure 5.17 presents the received signals measurement obtained from exposing all the channels to random phase delay perturbation. Such scenario can happen due to cables heating. Figure 5.18 shows the resulting simulated DOA estimation for this anomaly.

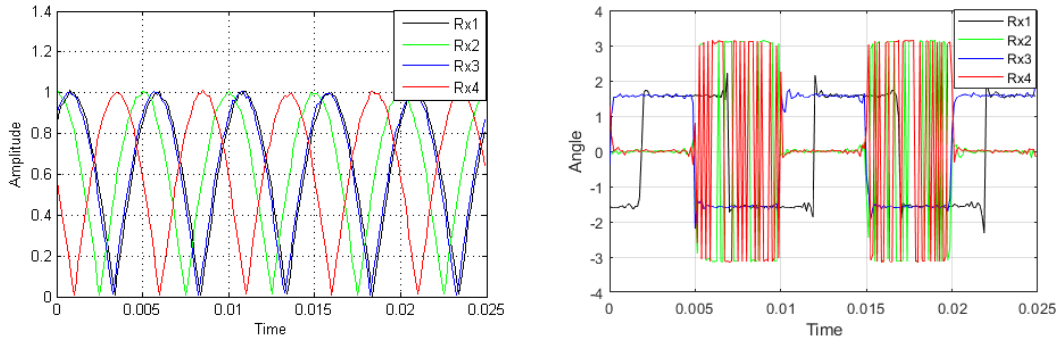

Figure 5.17: Received signals using a non-synchronized receiver, Scenario 2

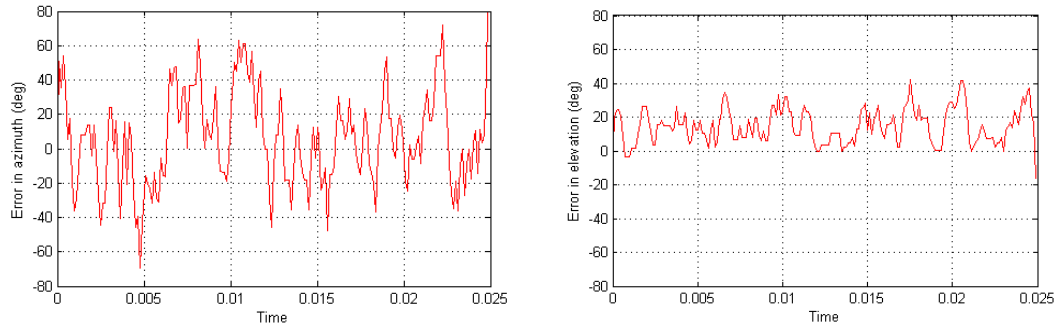

Figure 5.18: MUSIC DOA estimation error for phase perturbation, scenario 2

The above results were obtained with very minimum noise levels. It is very clear that this case by far is the worst between all other anomalies, which proves how critical is phase coherence for DF estimation.

5.4.3. ADC anomalies. Analog to digital converter anomalies include DC offset, sampling mismatching between channels, as well as quantization and encoding errors. Most of the suggested SDRs and RF receivers have embedded DC offset correction functionalities.

Figure 4.19 below shows how the performance of DF algorithm is degraded rapidly by having a sizable DC offset in the received signals.

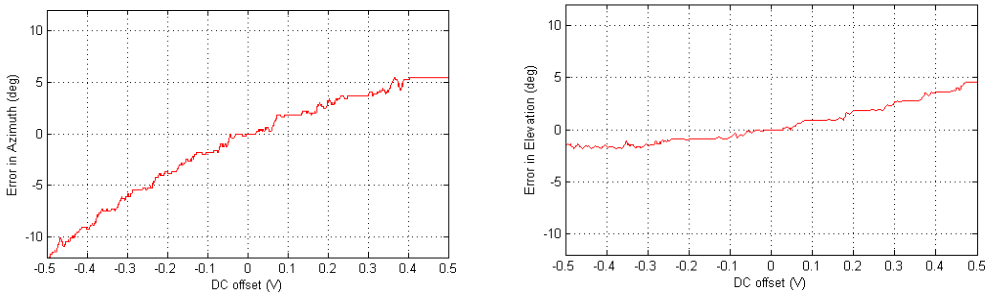

Figure 5.19: MUSIC DOA estimation error for DC offset anomaly

5.5. Moving Platform DOA Estimation

The objective of this study is to integrate the DF system on a mobile airborne platform. All the previous results are valid, even if the system is not mobile as well. This section simulates the DOA estimation technique for a moving UAV scenario with SNR = *1dB*. Figure 5.20 shows the estimated azimuth and elevation for this experiment, where the azimuth changes from *-40º* to *40º* while the elevation changes from *10º* to *80º*. Figure 5.21 displays the error in the simulated DOA estimation method.

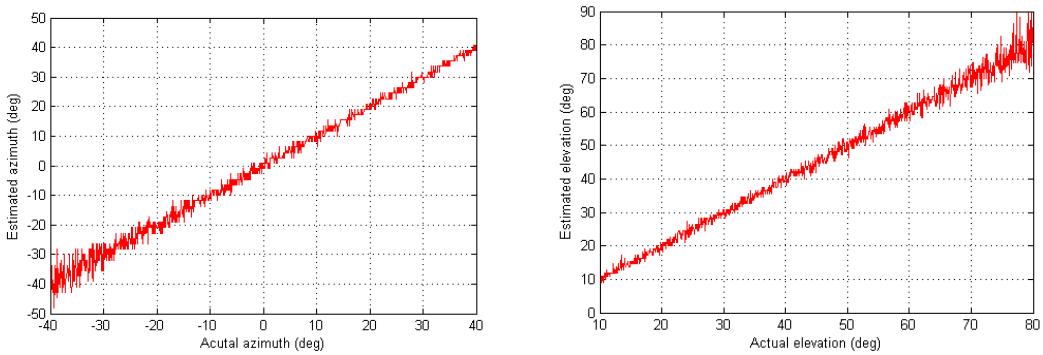

Figure 5.20: MUSIC DOA estimation for a moving platform

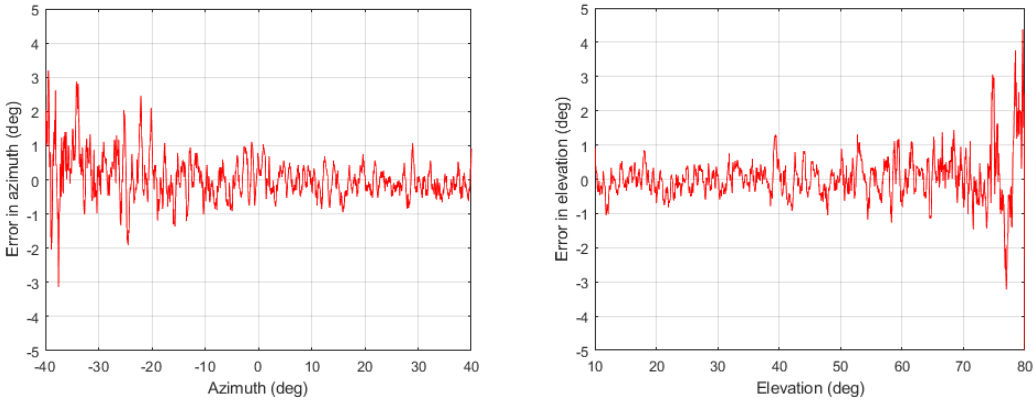

Figure 5.21: MUSIC DOA estimation error for a moving platform

We need to keep in mind that the MUSIC search limits are -90^o to 90^o in azimuth and 0^o to 90^o in elevation, as DOA out of these ranges will have incorrect measurement. That is why the error increases near the edges of the maximum range of angles.

5.6. Geolocation using DOA Estimation and Navigation System

In this section, the estimated DOA will be integrated with navigation data in order to geolocate a transmitting RF sources located at position (X_T, Y_T, Z_T). The source is assumed to be on sea level, which means its altitude $Z_T = 0$. Figure 5.22 shows a fixed-wing UAV simulated in flight gear simulator. As appears in the figure, the air traffic control tower of San Francisco International Airport, which will be assumed as the transmitting source we are trying to localize.

Figure 5.22: Scene of FlightGear flight simulator connected to Google maps

5.6.1. Fixed UAV. For a quadcopter drone that can maintain its position while flying, DOA estimation is much easier. The experiment results presented in Figure 5.23, assumed the UAV position is fixed at $(X_R, Y_R, Z_R) = (100,100,100)m$, and the source position is $(X_T, Y_T, Z_T) = (0,0,0)m$. Results obtained for a 4-element UCA at $10dB$ SNR.

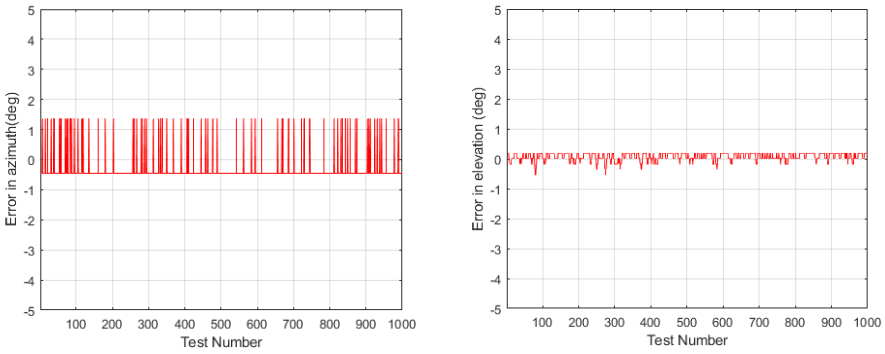

5.23. MUSIC DOA estimation error for a fixed airborne platform

Figure 5.24 shows the geographical position using the equations derived in Section 3.6. We need to address that for farther sources, a small deviation in the DOA can cause a huge error in the position estimation. It is important noting that MUSIC is not designed for range detection.

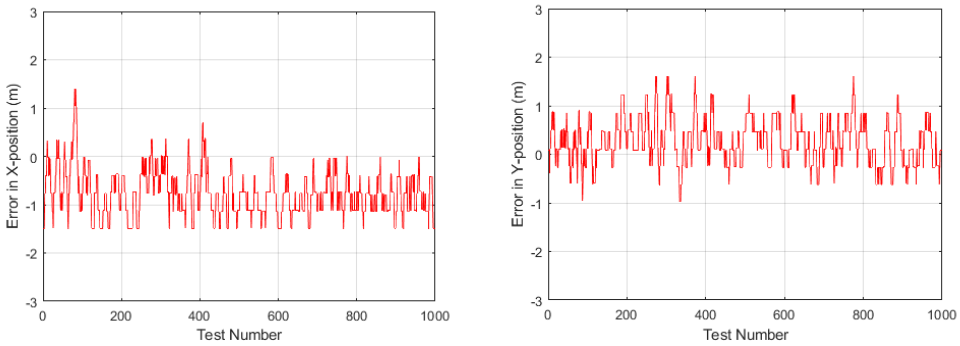

5.24. Position estimation error for a fixed airborne platform

5.6.2. Moving UAV. For a fixed-wing UAV such as the one shown in Figure 5.20, the fixed-position state can not be achieved. With the aid of Figure 5.25, this experiment simulates the geolocation of the control tower while the UAV moving above the tower. Figure 5.25 shows a UAV mission on QGroundControl ground station simulator. The mission starts from point $(X_R, Y_R, Z_R) = (100,100,1000)m$ to point $(0,100,1000)m$. The UAV should maintain the altitude heading to North, X-axis is assumed as the North, and Y-axis as the East in this scenario. The tower position is assumed at $(X_T, Y_T, Z_T) = (0,0,0)m$.

Figure 5.25: QGroundControl flight simulator and mission planning software

For this experiment, the altitude was set to *1000* meters to show how a small deviation in the DOA can affect the geolocation. The DF estimation results in Figure 5.26 are fairly accurate, with larger deviation when the azimuth is close to 0^o, which is expected from the MUSIC algorithm. However, for the geolocation results shown in Figure 5.27, the deviation is huge due to the high altitude of the UAV.

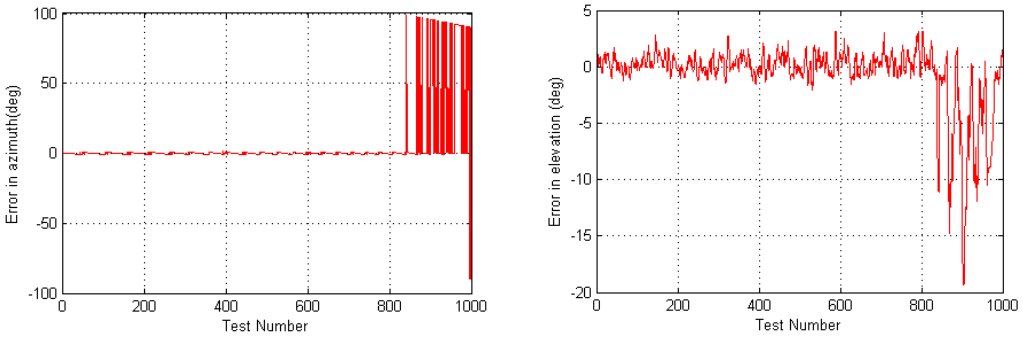

Figure 5.26: MUSIC DOA estimation error for a moving airborne platform

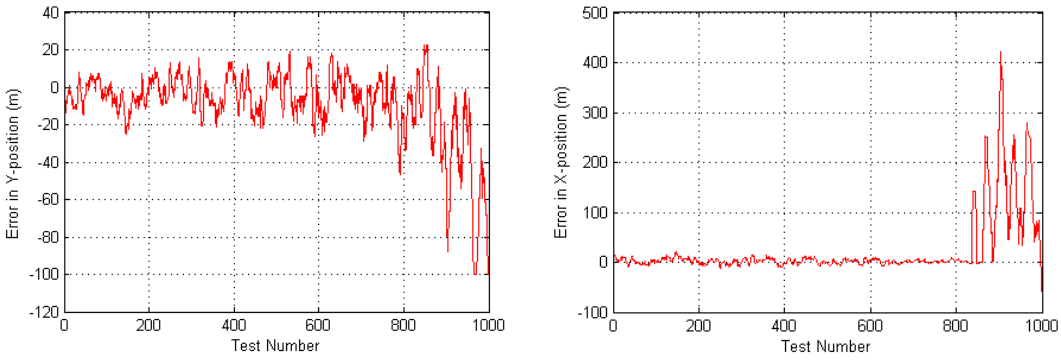

Figure 5.27: Position estimation error for a moving airborne platform

Chapter 6. Conclusion and Future Work

Nowadays, unmanned aerial vehicles (UAVs) are widely used in various civil and military applications. The rapid spread of UAVs use occured mainly due to their attractive features, such as the low cost, flexibility, and ease in operation and maintenance. The main objective of this research is to investigate several means to localize ground transmitters using a UAV-airborne antenna array.

In this thesis, direction finding (DF) systems were described and the guidelines for their design and implementation were stated in detail. Literature background of different types of DF systems was discussed, and DF applications in civil and military areas have been clearly presented. The thesis has highlighted the theory of passive DF using antenna arrays, as well as the theory of the phased antenna array that was comprehensively discussed. As examples, most common direction of arrival (DOA) estimation techniques and phase measurement algorithms were addressed and investigated.

The Multiple Signal Classification (MUSIC) DOA estimation method, as well as the inphase-quadrature (IQ) and discrete Fourier transform (DFT) phase measurement methods were investigated in various testing environments. Furthermore, hardware anomalies were clearly stated and intensely discussed, and their effects on the MUSIC DOA estimation method were presented in different scenarios, in order to measure the performance of the MUSIC algorithm, using results obtained by MATLAB computer simulation.

Hardware implementation requirements to integrate a DF system on a mobile platform was entirely discussed, and the guidelines to the system design, assembly, and implementation were stated. Some of the diverse DF solutions and hardware components and their characteristics were also presented to widen the scope of knowledge. Finally, the recommended hardware features and drawbacks have been presented and discussed.

As an outcome of simulation results, the MUSIC algorithm has proved to be a high-resolution DF method. However, its performance was observed to degrade rapidly with phase desynchronization. Moreover, it is computationally heavy, and it is

inconvenient to store its entire spectrum for UAV solutions. With limitation of resources, in order to implement the DF algorithm to be onboard, we recommend replacing the MUSIC algorithm with one of its less complicated versions, such as root-MUSIC.

Likewise, in order to accommodate a phase array antenna in a UAV, we have to care about the weight and size of that antenna, compared to the limited payload of most UAVs. The size of the antenna array is proportional to the wavelength of the targeted signals, and thus targeting low frequency transmitters will require a lager array, and hence a bigger UAV.

Future work includes acquiring the hardware equipment needed to implement the system, including the RF receiver, the digital signal processor, and the navigation system. Afterwards, the next step is hardware emulation with MATLAB or other software development tool, which provides signal processing techniques, such as GNU Radio. Finally, the system is to be integrated, and entirely tested before being deployed to the mission.

References

[1] S. Chandran, *Advances in Direction-of-Arrival Estimation*. Norwood, MA, USA: Artech House, 2006, pp. 3-19.

[2] P.J.D. Gething, *Radio Direction Finding and Super Resolution*. London: Peter Peregrimus Ltd, 1991, pp. 306-321.

[3] G.W. Osborne and L. Hardman, "Automatic direction finder sense antenna," U.S. Patent 5 353 038, Oct. 4, 1994.

[4] R. Zekavat and R. M. Buehrer, *Handbook of Position Location: Theory, Practice and Advances*. Piscataway, NJ, USA: IEEE Press, 2012, pp. 23-34.

[5] S. M. M. Dehghan and H. Moradi, "A new approach for simultaneous localization of UAV and RF sources (SLUS)," *2014 International Conference on Unmanned Aircraft Systems (ICUAS)*, Orlando, FL, 2014, pp. 744-749.

[6] S. Zorn, M. Gardill, R. Rose, A. Goetz, R. Weigel and A. Koelpin, "A smart jamming system for UMTS/WCDMA cellular phone networks for search and rescue applications," *2012 IEEE/MTT-S International Microwave Symposium Digest*, Montreal, QC, 2012, pp. 1-3.

[7] D. Tassetto, E. H. Fazli and M. Werner, "A Novel Hybrid Algorithm for Passive Localization of Victims in Emergency Situations," *2008 4th Advanced Satellite Mobile Systems*, Bologna, 2008, pp. 320-327.

[8] W. Abdessamad, Y. Nasser, H. Artail, S. Chazbek, G. Fakher and O. Bazzi, "An SDR platform using direction finding and statistical analysis for the detection of interferers," *2016 8th International Congress on Ultra Modern Telecommunications and Control Systems and Workshops (ICUMT)*, Lisbon, 2016, pp. 43-48.

[9] Anttila, D.S, "Adaptive radio direction finding system," U.S. Patent 5 448 248, Sep. 5, 1995.

[10] Yuanbo Xiong, Boon Poh Ng and R. Yang, "RF emitter localization and beam pattern auto-calibration using amplitude comparison of a two-element array," *2015 IEEE 6th International Workshop on Computational Advances in Multi-Sensor Adaptive Processing (CAMSAP)*, Cancun, 2015, pp. 313-316.

[11] L. G. Bullock, G. R. Oeh and J. J. Sparagna, "An Analysis of Wide-Band Microwave Monopulse Direction-Finding Techniques," *IEEE Transactions on Aerospace and Electronic Systems*, vol. AES-7, no. 1, pp. 188-203, Jan. 1971.

[12] B. M. Leiner, "An Analysis and Comparison of Energy Direction Finding Systems," *IEEE Transactions on Aerospace and Electronic Systems*, vol. AES-15, no. 6, pp. 861-873, Nov. 1979.

[13] E. Boch and M. Stapleton, "Direction-finding performance of a Ka-band ESM receiver," *IEEE Microwave and Guided Wave Letters*, vol. 4, no. 1, pp. 9-10, Jan. 1994.

[14] A.Q. Khan, M. Riaz and A. Bilal, "Various Types of Antenna with Respect to their Applications: A Review", *International Journal of Multidisciplinary Sciences and Engineering*, vol. 7, no. 3, pp. 1-8, Mar. 2016

[15] W. H. Kummer, "Basic array theory," *Proceedings of the IEEE*, vol. 80, no. 1, pp. 127-140, Jan. 1992.

[16] Z. Chen, G. K. Gokeda and Y. Yu, *Introduction to Direction-of-Arrival Estimation*, USA, MA, Norwood: Artech House, 2010.

[17] R. Pohlmann, S. Zhang, T. Jost and A. Dammann, "Power-based direction-of-arrival estimation using a single multi-mode antenna," *2017 14th Workshop on Positioning, Navigation and Communications (WPNC)*, Bremen, 2017, pp. 1-6.

[18] J. N. Ash and L. C. Potter, "Sensor network localization via received signal strength measurements with directional antennas" *Proc. Allerton Conference on Communication, Control, and Computing*, 2004, pp. 1861-1870.

[19] A. Cidronali, S. Maddio, G. Giorgetti and G. Manes, "Analysis and Performance of a Smart Antenna for 2.45-GHz Single-Anchor Indoor Positioning," *IEEE Transactions on Microwave Theory and Techniques*, vol. 58, no. 1, pp. 21-31, Jan. 2010.

[20] R. Schmidt, "Multiple Emitter Location and Signal Parameter Estimation," *IEEE Transactions on Antennas and Propagation*, vol. 34, no. 3, pp. 276-280, March 1986.

[21] Q. Liu, F. Yan, Y. Han, S. Liu and M. Jin, "Reduced-order root-MUSIC based on Schur spectral factorization," *2016 IEEE International Conference on Ubiquitous Wireless Broadband (ICUWB)*, Nanjing, 2016, pp. 1-3.

[22] M. Rubsamen and A. B. Gershman, "Root-music based direction-of-arrival estimation methods for arbitrary non-uniform arrays," *2008 IEEE International Conference on Acoustics, Speech and Signal Processing*, Las Vegas, NV, 2008, pp. 2317-2320.

[23] A. Barabell, "Improving the resolution performance of eigenstructure-based direction-finding algorithms," *ICASSP '83. IEEE International Conference on Acoustics, Speech, and Signal Processing*, Boston, Massachusetts, USA, 1983, pp. 336-339.

[24] M. Pesavento, A. B. Gershman, K. M. Wong and J. F. Bohme, "Direction finding in partly calibrated arrays composed of nonidentical subarrays: a computationally efficient algorithm for the rank reduction (RARE) estimator," *Proceedings of the 11th IEEE Signal Processing Workshop on Statistical Signal Processing (Cat. No.01TH8563)*, Singapore, 2001, pp. 536-539.

[25] S. A. Elkader, A. B. Gershman and K. M. Wong, "Rank Reduction Direction-of-Arrival Estimators with an Improved Robustness against Subarray Orientation Errors," *IEEE Transactions on Signal Processing*, vol. 54, no. 5, pp. 1951-1955, May 2006.

[26] R. Roy and T. Kailath, "ESPRIT-Estimation of Signal Parameters via Rotational Invariance Techniques," *IEEE Transactions on Acoustics, Speech, and Signal Processing*, vol. 37, no. 7, pp. 984-995, July 1989.

[27] Xiaofeng Gong, Yougen Xu, and Zhiwen Liu, "Quaternion ESPRIT for direction finding with a polarization sentive array," *2008 9th International Conference on Signal Processing*, Beijing, 2008, pp. 378-381.

[28] Yeo-Sun Yoon, L. M. Kaplan and J. H. McClellan, "TOPS: New DOA Estimator for Wideband Signals," *IEEE Transactions on Signal Processing*, vol. 54, no. 6, pp. 1977-1989, June 2006.

[29] D. E. Lake, "Harmonic phase coupling for battlefield acoustic target identification," *Proceedings of the 1998 IEEE International Conference on Acoustics, Speech and Signal Processing, ICASSP '98 (Cat. No.98CH36181)*, Seattle, WA, USA, 1998, pp. 2049-2052 vol.4.

[30] P. S. Naidu, *Modern Digital Signal Processing: An Introduction*. Oxford, UK: Alpha Science Intl Ltd, 2003, pp. 29–31

[31] K. M. Ibrahim and M. A. H. Abdul-Karim, "A Novel Digital Phase Meter," *IEEE Transactions on Instrumentation and Measurement*, vol. IM-36, no. 3, pp. 711-716, Sep. 1987.
[32] M. F. Wagdy and M. S. P. Lucas, "Errors in Sampled Data Phase Measurement," *IEEE Transactions on Instrumentation and Measurement*, vol. IM-34, no. 4, pp. 507-509, Dec. 1985.
[33] S. M. Mahmud, "High Precision Phase Measurement using Adaptive Sampling," *IEEE Transactions on Instrumentation and Measurement*, vol. 38, no. 5, pp. 954-960, Oct. 1989.
[34] Micheletti, "Phase Angle Measurement between two Sinusoidal Signals," *IEEE Transactions on Instrumentation and Measurement*, vol. 40, no. 1, pp. 40-42, Feb. 1991.
[35] P. D. Groves, "Principles of GNSS, Inertial, and Multisensor Integrated Navigation Systems, 2nd edition [Book review]," *IEEE Aerospace and Electronic Systems Magazine*, vol. 30, no. 2, pp. 26-27, Feb. 2015.
[36] W. M. F. Al-Masri, M. F. Abdel-Hafez and M. A. Jaradat, "Inertial Navigation System of Pipeline Inspection Gauge," *IEEE Transactions on Control Systems Technology*, vol. 28, no. 2, pp. 609-616, March 2020.
[37] Nath, N.P., Parija, S.R., Sahu, P.K. and Singh, "Survey Paper: Location Management in CDMA Network," *International Journal of Grid and Distributed Computing*, vol. 8, pp.287-298, 2015.
[38] A. Noureldin, T. B. Karamat and J. Georgy, *Fundamentals of Inertial Navigation Satellite-Based Positioning and Their Integration*, Berlin, Germany: Springer Science and Business Media, 2012.
[39] W. M. Al-Masri, "Inertial Navigation System of In-Pipe Robot," Master of Science Thesis, American University of Sharjah, United Arab Emirates, 2016.
[40] R. Faragher, "Understanding the Basis of the Kalman Filter Via a Simple and Intuitive Derivation [Lecture Notes]," *IEEE Signal Processing Magazine*, vol. 29, no. 5, pp. 128-132, Sept. 2012.
[41] James R. Clynch, *Earth Coordinates*, Electronic Documentation, Feb. 2006.
[42] K. M. Saadeddin, "Estimating Vehicle State by GPS/IMU Fusion with Vehicle Dynamics," Master of Science Thesis, American University of Sharjah, United Arab Emirates, 2013.
[43] Andrea Civita, "A Mobile Acquisition System and a Method for Hips Sway Fluency Assessment", Internet: www.researchgate.net/figure/An-illustration-of-the-three-angles-yaw-pitch-and-roll-returned-by-the-Hyper-IMU_fig1_329603549, Dec. 12, 2018 [Dec 12, 2020]
[44] P. McBride, "Beyond Orwell: The Application of Unmanned Aircraft Systems in Domestic Surveillance Operations", *J. Air L. & Com.*, vol. 74, pp. 627, 2009.
[45] S. Appadwedula and C. M. Keller, "Direction-finding results for a vector sensor antenna on a small UAV," *Fourth IEEE Workshop on Sensor Array and Multichannel Processing*, Waltham, MA, 2006, pp. 74-78.
[46] K. P. Valavanis and G. J. Vachtsevanos, "UAV applications: Introduction" in *Handbook of Unmanned Aerial Vehicles*, Dordrecht, The Netherlands: Springer, 2015, pp. 2639-2641.
[47] S. Häfner, M. Käske, R. Thomä, "On Calibration and Direction Finding with Uniform Circular Arrays", *International Journal of Antennas and Propagation*, vol. 2019, pp. 1-12, Jul. 2019.

[48] Mount Diablo Amateur Radio Club, "Coaxial Cable and Ladder Line," Internet: www.mdarc.org/resources/technical/coax-ladder, Feb 2016 [Dec. 12, 2020].
[49] Analog Devices, "AD9361 Data Sheet (Rev. F), RF Agile Transceiver," Internet: www.analog.com/en/products/ad9361.html, 2016 [Dec. 12, 2020].
[50] D. Pu, A. Cozma and T. Hill, "Four Quick Steps to Production: Using Model-Based Design for Software-Defined Radio (Part 1)," Internet: www.analog.com/en/analog-dialogue/articles/using-model-based-design-sdr-2.html, Sep 2015 [Dec. 12, 2020].
[51] Analog Devices, "AD-FMCOMMS5-EBZ User Guide," Internet: www. https://wiki.analog.com/%20resources/eval/user-guides/ad-fmcomms5-ebz", May 2019 [Dec 12, 2020].
[52] Analog Devices, "AD9371 Data Sheet (Rev.B), Integrated, Dual RF Transceiver with Observation Path", Internet: www.analog.com/en/products/ad9371.html#:~:text=The%20AD9371%20is%20a%20highly,and%20digital%20signal%20processing%20functions, 2017 [Dec. 12, 2020].
[53] M. T. d. Oliveira, R. K. Miranda, J. P. C. da Costa, A. L. de Almeida, and R. T. d. Sousa, "Low Cost Antenna Array Based Drone Tracking Device for Outdoor Environments," *Wireless Communications and Mobile Computing*, vol. 2019, pp. 1-14, Jan 2019.
[54] Ancortek, "SDR 2400T2R4 Datasheet," Internet: www.ancortek.com/wp-content/uploads/2020/05/SDR-2400T2R4-Datasheet.pdf, 2020 [Dec. 12, 2020].
[55] RTL-SDR, "Kerberossdr - 4 Coherent Channels RF Receiver," Internet: www.rtl-sdr.com/ksdr, Feb 2019 [Dec. 12, 2020].

Vita

Mirghani Moutaman was born in 1992, in Tripoli, Libya. He received his primary and secondary education in Khartoum, Sudan. He received his B.Sc. degree in Electrical and Electronic Engineering from the University of Khartoum in 2014. From 2015 to 2017, he worked as an Embedded Systems Engineer in Badr Technology Corporation.

In January 2017, he joined the Mechatronics Engineering master's program in the American University of Sharjah as a graduate teaching assistant. During his master's study, he co-authored 1 paper which was presented in national conferences. His research interests are in (embedded systems, robotics, digital signal processing, and artificial intelligence).